mathematics

MDPI

Article

In-Plane Vibrations of Elastic Lattice Plates and Their Continuous Approximations

Noël Challamel [1,*], Huu Phu Nguyen [2], Chien Ming Wang [2] and Giuseppe Ruta [3]

[1] Centre de Recherche, Université Bretagne Sud, IRDL (CNRS UMR 6027), Rue de Saint Maudé, BP92116, 56321 Lorient Cedex, France
[2] School of Civil Engineering, University of Queensland, St Lucia, QLD 4072, Australia; huuphu.nguyen@uq.edu.au (H.P.N.); cm.wang@uq.edu.au (C.M.W.)
[3] Dipartimento D'Ingegneria Strutturale e Geotecnica, Universitá "La Sapienza", 00185 Roma, Italy; giuseppe.ruta@uniroma1.it
* Correspondence: noel.challamel@univ-ubs.fr

Abstract: This paper presents an analytical study on the in-plane vibrations of a rectangular elastic lattice plate. The plane lattice is modelled considering central and angular interactions. The lattice difference equations are shown to coincide with a spatial finite difference scheme of the corresponding continuous plate. The considered lattice converges to a 2D linear isotropic elastic continuum at the asymptotic limit for a sufficiently small lattice spacing. This continuum has a free Poisson's ratio, which must be lower than that foreseen by the rare-constant theory, to preserve the definite positiveness of the associated discrete energy. Exact solutions for the in-plane eigenfrequencies and modes are analytically derived for the discrete plate. The stiffness characterising the lattice interactions at the boundary is corrected to preserve the symmetry properties of the discrete displacement field. Two classes of constraints are considered, i.e., sliding supports at the nodes, one normal and the other parallel to the boundary. For both boundary conditions, a single equation for the eigenfrequency spectrum is derived, with two families of eigenmodes. Such behaviour of the lattice plate is like that of the continuous plate, the eigenfrequency spectrum of which has been given by Rayleigh. The convergence of the spectrum of the lattice plate towards the spectrum of the continuous plate from below is confirmed. Two continuous size-dependent plate models, considering the strain gradient elasticity and non-local elasticity, respectively, are built from the lattice difference equations and are shown to approximate the plane lattice accurately.

Keywords: lattice/discrete elasticity; continuum elasticity; elastodynamics; difference equations; partial differential equations; in-plane vibrations; eigenvalue problem; discrete plate

MSC: 34A33; 34K31; 37K60; 39A36; 52C05; 74B05; 74H45; 70J10; 34C46

check for updates

Citation: Challamel, N.; Nguyen, H.P.; Wang, C.M.; Ruta, G. In-Plane Vibrations of Elastic Lattice Plates and Their Continuous Approximations. *Mathematics* **2024**, *12*, 2312. https://doi.org/10.3390/math12152312

Academic Editor: Alberto Ferrero

Received: 28 June 2024
Revised: 16 July 2024
Accepted: 19 July 2024
Published: 24 July 2024

Copyright: © 2024 by the authors. Licensee MDPI, Basel, Switzerland. This article is an open access article distributed under the terms and conditions of the Creative Commons Attribution (CC BY) license (https://creativecommons.org/licenses/by/4.0/).

1. Introduction

This paper presents new solutions for the in-plane vibration problems of two-dimensional rectangular linear elastic lattices. The exact solution of this discrete problem is connected to that of a continuous plate, obtained at the asymptotic limit for an infinite number of particles in each direction. Bridging discrete and continuous elasticity is an old problem of mechanics that emerged during the 19th century with the so-called molecular foundation of elasticity (see the historical analysis of Capecchi et al., 2010, [1] Capecchi et al., 2011 [2] or Challamel et al., 2023 [3]). This problem of bridging discrete to continuous elasticity is still active nowadays, and the problem also includes the development of generalised continuum elasticity (Andrianov et al., 2021 [4]; dell'Isola and Steigmann, 2020 [5]; Wang et al., 2020 [6]).

Although many solutions are available for 1D lattices since the solution obtained by Lagrange (1759) [7,8] for the eigenfrequencies of a fixed–fixed lattice string (mathematically equivalent to a lattice rod), the exact solutions for the free vibration of 2D or 3D finite elastic

lattices are not so well documented in the literature. There are reference solutions for the out-of-plane vibration of lattice membranes and plates. Rosenau (1987) [9], Andrianov and Awrejcewicz (2008) [10], Lombardo and Askes (2010) [11] and Hérisson et al. (2018) [12] obtained the exact wave dispersive equation in the infinite lattice membrane. Rosenau (1987) [9] also derived a lattice-based continuous nonlocal membrane model, by using the Padé approximant of the associated pseudodifferential operator of the discrete lattice. The eigenfrequencies of a fixed–fixed rectangular lattice membrane (finite lattice membrane) have been analytically found by Hérisson et al. (2018) [12] from the resolution of a linear difference eigenvalue problem. This approach is mathematically equivalent to the finite difference (FD) formulation of the continuous membrane problem, regarding which the exact discrete resolution was already presented by Chen (1971) [13] and Tong et al. (1971) [14]. Hérisson et al. (2018) [12] also investigated the efficiency of the nonlocal continuous membrane model pioneered by Rosenau (1987) [9] for approximating the eigenfrequency of the fixed–fixed lattice membrane.

Zhang et al. (2015) [15] studied analytically the free vibration of simply supported lattice rectangular plates (discrete Kirchhoff–Love plate model) and derived natural frequencies as exact solutions of the associated linear difference eigenvalue problem. As the mathematical problem is equivalent to the finite difference (FD) formulation of a continuous Kirchhoff–Love plate, the eigenfrequencies of the simply supported lattice plate coincide with those derived exactly from the FD scheme by Chen (1971) [13]. Wang et al. (2020) [6] gave exact solutions for lattice plates with various constraints (including Levy-type boundary conditions), thus generalising the solution of Chen (1971) [13] and Zhang et al. (2015) [15], that has been restricted to Navier-type boundary conditions. Challamel et al. (2016) [16] and Hache et al. (2017) [17] (see also Challamel et al., 2021 [18]) derived a gradient and a nonlocal continuum Kirchhoff–Love plate model from the lattice plate model and compared the higher-order solutions to the lattice one for simply supported boundary conditions. These two structural cases of out-of-plane vibration of a discrete membrane and plate are 2D one-field discrete problems, i.e., with only one kinematic field for the unknown displacement.

To the authors' knowledge, there is no analogous result for in-plane 2D/3D finite lattices described by a two-field or a three-field unknown displacement. Most results available in the literature for in-plane 2D or 3D lattices hold for infinite media, for which the dispersion response has been analytically characterised (Born and von Kármán, 1912 [19]; Gazis et al., 1960 [2]; Challamel et al., 2023 [3]). Born and von Kármán (1912) [19] first introduced the mixed differential-difference equations of a cubic lattice with central and non-central interactions. They also derived the wave dispersive property in an infinite Lagrange lattice, and in infinite 3D lattices [19]. The non-central interactions considered by Born and von Kármán [19] are of the shear type, which have been shown later to violate the rotation invariance principle (the conditions for rotational invariance of lattices were extensively studied during the 1960s by Lax, 1965 [20], Gazis and Wallis, 1966 [21], Keating, 1966 [22] and Keating, 1966 [23]). Gazis et al. (1960) [24] obtained the mixed differential-difference equations of a cubic lattice with central and non-central (angular-type) interactions, consistent with the rotation invariance principle. The mixed differential-difference equations derived by Gazis et al. [20] differ from the ones of Born and von Kármán [19], as shown by Challamel et al. [3] for 2D or 3D lattices. Gazis et al. [20] also analytically characterised the wave dispersive behaviour of such infinite lattice. To the authors' knowledge, the exact solutions for the vibrations of finite cubic lattices with central and angular interactions have not been derived in the literature.

The paper is focused on the analytical determination of the in-plane eigenfrequencies of a rectangular lattice (2D lattice). The lattice considered herein is the cubic lattice introduced by Gazis et al. (1960) [24]. This lattice exhibits central and non-central interactions that make it possible to calibrate the macroscopic elastic parameters for a wide range (see the discussion in Challamel et al., 2023 [3] and Challamel et al., 2024 [25]). Gazis et al. (1960) [24] already obtained the exact dispersive curves of their lattice in the case of infinite media. Mindlin (1968) [26] expanded the difference equations of Gazis et al.'s [23]

lattice and obtained a lattice-based gradient elasticity model, if second-order terms are included. Mindlin (1970) [27] obtained exact solutions for Gazis' type of finite lattices for four problems: thickness-shear vibration of a plane lattice; face-shear and thickness-twist waves in a plate; axial shear vibration and, in the end, the torsion of a rectangular bar. The first three are reduced to a one-dimensional eigenfrequency problem, whereas the last one is a static problem. The present paper is restricted to a linear vibration analysis, due to the linearity behaviour in each periodic lattice cell. We do not explore the vibration behaviour of nonlinear elastic lattices, as initially studied by Fermi et al. (1955) [28] for a one-dimensional periodic lattice with a nonlinear restoring force. The nonlinear lattice of Fermi et al. (1955) [28] initiated some new research areas in the field of nonlinear wave propagation and soliton theory (Weissert, 1997 [29]; Dauxois et al., 2005 [30]; Dauxois and Peyrard, 2006 [31] or more recently Vainchtein, 2022 [32]). The papers of Potapov et al. (2002) [33] or Friesecke and Matthies (2003) [34] on solitary waves in 2D lattices may be mentioned for 2D nonlinear lattices, where the interactions have been restricted to the central type.

In this paper, the in-plane vibration of a rectangular linear elastic lattice according to the model by Gazis et al. [24], in which non-central interactions are of the angular type, is investigated to obtain the exact solutions for the eigen-frequencies and modes analytically, for simply supported boundary conditions (in-plane vibration problem with sliding supports). This lattice problem (discrete problem) has not been solved analytically in the literature. The free vibration characteristics of the rectangular lattice are obtained by posing and solving a linear two-field difference eigenvalue problem. The stiffness of the lattice interactions in the vicinity of the boundary is corrected to preserve the symmetry properties of the discrete displacement field along the boundaries. Two classes of constraints are considered, i.e., sliding supports at the nodes, once normal and then parallel to the boundary. For both boundary conditions, a single equation for the eigenfrequency spectrum is derived, with two families of eigenmodes. The lattice solution is compared to the available continuous one of the in-plane eigenfrequency for a plate, analytically derived by Rayleigh (1894) [35] (see also Rayleigh, 1889 [36]), and numerically obtained by Bardell et al. (1996) [37] and Gorman (2006) [38]. We also derived higher-order continuum plate models, under plane stress assumptions, which are asymptotically formulated from the lattice plate difference equations. It is possible to obtain the exact solutions of the eigenfrequencies for both higher-order plate models, a strain gradient elasticity plate model and a nonlocal plate model. The strain gradient plate model is similar to the one derived by Mindlin (1968) [26], here restricted to plane stress assumptions. Both higher-order continua are shown to accurately fit the behaviour of the lattice, including its scale-dependence behaviour, i.e., the dependence of the normalised eigenfrequency with respect to the number of cells in each direction. Both models converge towards the local plate solution derived by Rayleigh (1894) [35] when the number of cells in each direction is sufficiently large.

2. In-Plane Vibrations of a Discrete Rectangular Plate

We investigated the free vibration of a 2D linear elastic lattice exhibiting central and non-central angular interactions (see Figure 1). This lattice is the one pioneered by Gazis et al. (1960) [24] for cubic lattices with angular interactions, which has also been studied by Mindlin (1968) [26] and Mindlin (1970) [27]. This lattice, restricted to a 2D analysis in this study, is monatomic and square, composed of particles with an equal mass M and lattice spacing a. The linear elastic interactions among them consist of (a) nearest and next-to-nearest central forces, represented by axial springs of stiffness α and β between the nearest and next-to-nearest particles, respectively; (b) non-central interactions given by force couples, represented by rotational springs of stiffness $C = \gamma\, a^2$. α and β are the two parameters of the central interaction, whereas γ is the parameter of the non-central (or angular) interaction. The three stiffness parameters α, β and γ have the same dimensions. The governing equations of the lattice may be derived from the elastic potential energy.

$$
\begin{aligned}
U = &\sum_i \sum_j \frac{\alpha}{4}\left[\left(u_{i+1,j}-u_{i,j}\right)^2+\left(u_{i+1,j+1}-u_{i,j+1}\right)^2+\left(v_{i,j+1}-v_{i,j}\right)^2+\left(v_{i+1,j+1}-v_{i+1,j}\right)^2\right] \\
&+\frac{\beta}{4}\left[\left(u_{i+1,j+1}-u_{i,j}+v_{i+1,j+1}-v_{i,j}\right)^2+\left(u_{i+1,j}-u_{i,j+1}-v_{i+1,j}+v_{i,j+1}\right)^2\right] \\
&+\frac{1}{2}\gamma\left[\begin{array}{l}\left(u_{i,j+1}-u_{i,j}+v_{i+1,j}-v_{i,j}\right)^2+\left(u_{i+1,j+1}-u_{i+1,j}+v_{i+1,j}-v_{i,j}\right)^2 \\ +\left(u_{i,j+1}-u_{i,j}+v_{i+1,j+1}-v_{i,j+1}\right)^2+\left(u_{i+1,j+1}-u_{i+1,j}+v_{i+1,j+1}-v_{i,j+1}\right)^2\end{array}\right]
\end{aligned}
\tag{1}
$$

where the stiffnesses α, β, γ are positive to ensure the positive definiteness of the energy; pure central interactions are attained if $\gamma = 0$ (Navier's, Poisson's or Cauchy's molecular assumption).

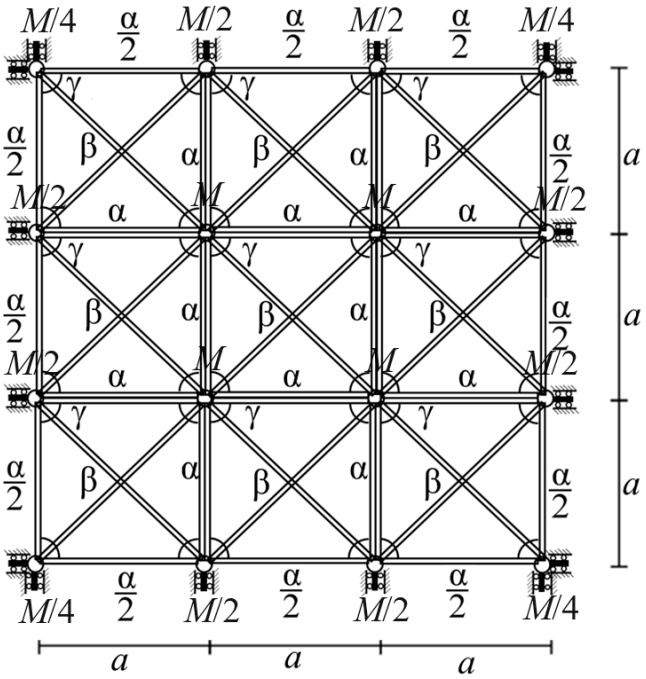

Figure 1. Lattice plate with central and angular interactions on sliding support (case A); $n = m = 3$; corrections of the elastic interactions at the border.

Since the lattice has concentrated masses only, its kinetic energy has the simple form:

$$
T = \sum_i \sum_j \frac{1}{2} M\, \dot{u}_{i,j}^2 + \frac{1}{2} M\, \dot{v}_{i,j}^2 \tag{2}
$$

where the superdot denotes the time derivative. Hamilton's principle applied to the Lagrangian $L = T - U$ yields the mixed differential-difference equations of the 2D Gazis et al.'s lattice (Challamel et al., 2022 [39]):

$$
\left\{\begin{array}{l}
\alpha\left(u_{i+1,j}-2u_{i,j}+u_{i-1,j}\right)+\frac{\beta}{2}\left(u_{i+1,j+1}+u_{i-1,j-1}+u_{i-1,j+1}+u_{i+1,j-1}-4u_{i,j}\right)+ \\
\left(\frac{\beta}{2}+\gamma\right)\left(v_{i+1,j+1}-v_{i-1,j+1}-v_{i+1,j-1}+v_{i-1,j-1}\right)+4\gamma\left(u_{i,j+1}-2u_{i,j}+u_{i,j-1}\right)=M\,\ddot{u}_{i,j} \\
\alpha\left(v_{i,j+1}-2v_{i,j}+v_{i,j-1}\right)+\frac{\beta}{2}\left(v_{i+1,j+1}+v_{i-1,j-1}+v_{i-1,j+1}+v_{i+1,j-1}-4v_{i,j}\right)+ \\
\left(\frac{\beta}{2}+\gamma\right)\left(u_{i+1,j+1}-u_{i-1,j+1}-u_{i+1,j-1}+u_{i-1,j-1}\right)+4\gamma\left(v_{i+1,j}-2v_{i,j}+v_{i-1,j}\right)=M\,\ddot{v}_{i,j}
\end{array}\right. \tag{3}
$$

If n, m are integers, we calculate the in-plane eigenfrequencies of rectangular lattices of length $L_1 = na$ along the 'horizontal' and width $L_2 = ma$ along the 'vertical' with sliding supports at their boundaries. In Figure 1, for instance, the lattice plate on sliding supports is represented with $n = m = 3$. Then, if ω is the circular frequency of the in-plane natural vibration, the mixed differential-difference equation, Equation (3), is reduced to a system of

spatial difference equations. We must solve the linear eigenvalue problem resulting from the coupled system of difference equations

$$\begin{cases} \alpha\left(u_{i+1,j}-2u_{i,j}+u_{i-1,j}\right)+\frac{\beta}{2}\left(u_{i+1,j+1}+u_{i-1,j-1}+u_{i-1,j+1}+u_{i+1,j-1}-4u_{i,j}\right)+ \\ \left(\frac{\beta}{2}+\gamma\right)\left(v_{i+1,j+1}-v_{i-1,j+1}-v_{i+1,j-1}+v_{i-1,j-1}\right)+4\gamma\left(u_{i,j+1}-2u_{i,j}+u_{i,j-1}\right)+M\omega^2u_{i,j}=0 \\ \alpha\left(v_{i,j+1}-2v_{i,j}+v_{i,j-1}\right)+\frac{\beta}{2}\left(v_{i+1,j+1}+v_{i-1,j-1}+v_{i-1,j+1}+v_{i+1,j-1}-4v_{i,j}\right)+ \\ \left(\frac{\beta}{2}+\gamma\right)\left(u_{i+1,j+1}-u_{i-1,j+1}-u_{i+1,j-1}+u_{i-1,j-1}\right)+4\gamma\left(v_{i+1,j}-2v_{i,j}+v_{i-1,j}\right)+M\omega^2v_{i,j}=0 \end{cases} \quad (4)$$

We consider two cases of constraints (which can be referred to as simply supported boundary conditions) provided by sliding supports at the boundary particles, as discussed, for instance, by Gorman (2006) [38] for a continuum in the shape of a plate:

- In case A (Figure 1), the tangential displacement and the normal load at the lattice boundary vanish (sliding supports normal to the boundary). The displacement-based boundary conditions are as follows:

$$v_{0,j}=0 \text{ for } j\in\{0,1,\ldots,m\};\ v_{n,j}=0 \text{ for } j\in\{0,1,\ldots,m\};$$

$$u_{i,0}=0 \text{ for } i\in\{0,1,\ldots,n\};\ u_{i,m}=0 \text{ for } i\in\{0,1,\ldots,n\}; \quad (5)$$

The discrete Dirichlet boundary conditions in Equation (5) for the simply supported edges (case A) are completed by the discrete Neumann boundary conditions of vanishing normal force along the four edges. The same boundary conditions of case A can be considered for the continuous plate, as shown in Figure 2.

- In case B (Figure 3), the normal displacement and the tangential load at the lattice boundary vanish (sliding supports parallel to the boundary).

$$u_{0,j}=0 \text{ for } j\in\{0,1,\ldots,m\};\ u_{n,j}=0 \text{ for } j\in\{0,1,\ldots,m\};$$

$$v_{i,0}=0 \text{ for } i\in\{0,1,\ldots,n\};\ v_{i,m}=0 \text{ for } i\in\{0,1,\ldots,n\}; \quad (6)$$

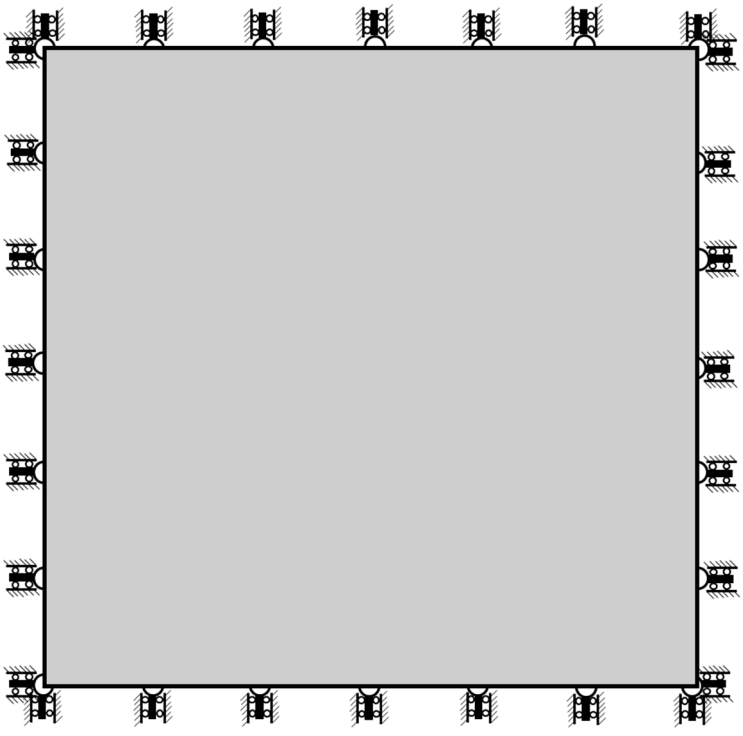

Figure 2. Continuous plate on sliding support (for the in-plane continuous plate problem)—case A.

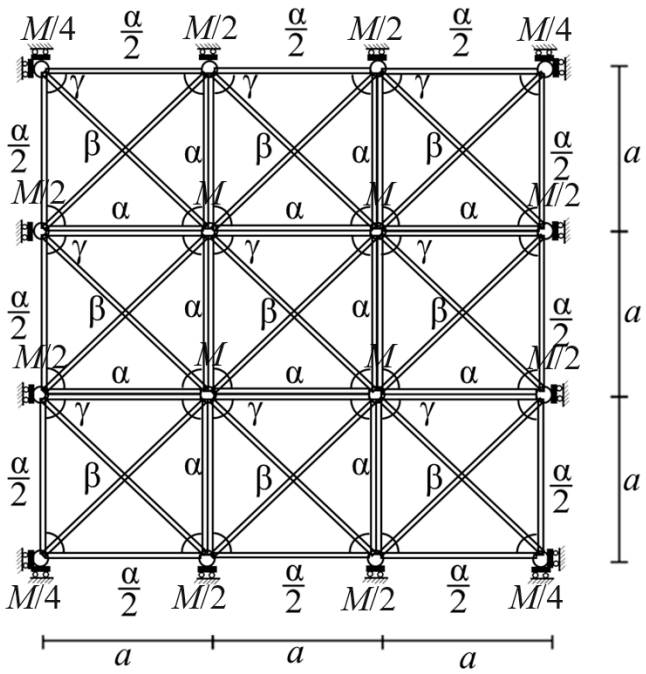

Figure 3. Lattice with central and angular interactions on sliding support (case B); $n = m = 3$; corrections of the elastic interactions at the border.

The discrete Dirichlet boundary conditions in Equation (6) of simply supported edges (case B) are completed by the discrete Neumann boundary conditions of vanishing of the tangential force along the four edges. The same boundary conditions of case B can be considered for the continuous plate, as shown in Figure 4.

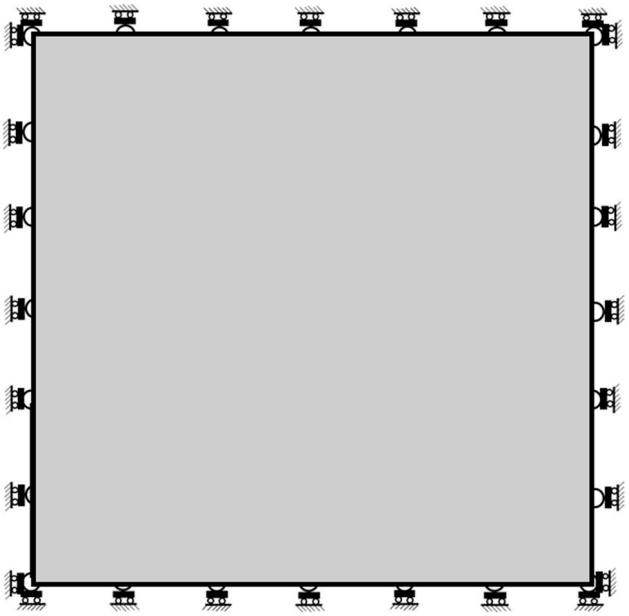

Figure 4. Continuous plate on sliding support (for the in-plane continuous plate problem)—case B.

As shown in Figures 1 and 3 for a square lattice with $n = m = 3$, the stiffness of border springs is half of that for the inner springs, as detailed by McHenry (1943) [40] and Hrennikoff (1941) [41] for 2D lattices with pure central interactions; we used the same approach in Challamel et al. (2023) [3] and Challamel et al. (2024) [25] to obtain the static responses of Gazis et al.'s lattices with central and non-central interactions. We follow here the same methodology for the free in-plane vibration of such lattices: the

eigenfrequencies and eigenmodes derive from the linear algebraic problem associated with the discrete displacement (standard matrix eigenvalue problem), and the stiffness and the mass matrices are assembled from the difference equation, Equation (4).

Additionally, some exact solutions can be obtained for the eigenfrequencies and eigenmodes of the $(n \times m)$ rectangular lattice supported as in cases A and B. Using a methodology described by Mindlin (1970) [27] for the free shear vibration of Gazis et al.'s lattice, and posing the (k_1, k_2) mode numbers, the solution for case A simply supported edges (with sliding normal to the boundary) is thought to be in the form:

$$u_{i,j} = U\cos\left(\frac{k_1\pi ai}{L_1}\right)\sin\left(\frac{k_2\pi aj}{L_2}\right) = U\cos\left(\frac{k_1\pi\, i}{n}\right)\sin\left(\frac{k_2\pi\, j}{m}\right)$$

$$\text{for } i \in \{0,1,\ldots,n\} \text{ and } j \in \{0,1,\ldots,m\}$$

$$\text{and } v_{i,j} = V\sin\left(\frac{k_1\pi ai}{L_1}\right)\cos\left(\frac{k_2\pi aj}{L_2}\right) = V\sin\left(\frac{k_1\pi\, i}{n}\right)\cos\left(\frac{k_2\pi\, j}{m}\right)$$

$$\text{for } i \in \{0,1,\ldots,n\} \text{ and } j \in \{0,1,\ldots,m\} \tag{7}$$

Similarly, the solution for case B simply supported edges (with sliding support along the boundary) is thought to be in the form:

$$u_{i,j} = U\sin\left(\frac{k_1\pi ai}{L_1}\right)\cos\left(\frac{k_2\pi aj}{L_2}\right) = U\sin\left(\frac{k_1\pi\, i}{n}\right)\cos\left(\frac{k_2\pi\, j}{m}\right)$$

$$\text{for } i \in \{0,1,\ldots,n\} \text{ and } j \in \{0,1,\ldots,m\}$$

$$\text{and } v_{i,j} = V\cos\left(\frac{k_1\pi ai}{L_1}\right)\sin\left(\frac{k_2\pi aj}{L_2}\right) = V\cos\left(\frac{k_1\pi\, i}{n}\right)\sin\left(\frac{k_2\pi\, j}{m}\right)$$

$$\text{for } i \in \{0,1,\ldots,n\} \text{ and } j \in \{0,1,\ldots,m\} \tag{8}$$

For both simply supported lattice plate problems with case A and case B boundary conditions, the substitution of Equation (7) into Equation (4) or the substitution of Equation (8) into Equation (4) furnishes:

$$\begin{cases} \left[4\alpha\sin^2\left(\frac{k_1\pi}{2n}\right) + 2\beta\left[1-\cos\left(\frac{k_1\pi}{n}\right)\cos\left(\frac{k_2\pi}{m}\right)\right] + 16\gamma\sin^2\left(\frac{k_2\pi}{2m}\right) - M\omega^2\right]U \\ +\left[(2\beta+4\gamma)\sin\left(\frac{k_1\pi}{n}\right)\sin\left(\frac{k_2\pi}{m}\right)\right]V = 0 \\ \left[(2\beta+4\gamma)\sin\left(\frac{k_1\pi}{n}\right)\sin\left(\frac{k_2\pi}{m}\right)\right]U \\ +\left[4\alpha\sin^2\left(\frac{k_2\pi}{2m}\right) + 2\beta\left[1-\cos\left(\frac{k_1\pi}{n}\right)\cos\left(\frac{k_2\pi}{m}\right)\right] + 16\gamma\sin^2\left(\frac{k_1\pi}{2n}\right) - M\omega^2\right]V = 0 \end{cases} \tag{9}$$

which can be rewritten as:

$$\begin{cases} A_{11}(\omega^2)\,U + A_{12}V = 0 \\ A_{21}U + A_{22}(\omega^2)\,V = 0 \end{cases} \tag{10}$$

with:

$$\begin{cases} A_{11}(\omega^2) = 4\alpha\sin^2\left(\frac{k_1\pi}{2n}\right) + 2\beta\left[1-\cos\left(\frac{k_1\pi}{n}\right)\cos\left(\frac{k_2\pi}{m}\right)\right] + 16\gamma\sin^2\left(\frac{k_2\pi}{2m}\right) - M\omega^2 \\ A_{21} = A_{12} = (2\beta+4\gamma)\sin\left(\frac{k_1\pi}{n}\right)\sin\left(\frac{k_2\pi}{m}\right) \\ A_{22}(\omega^2) = 4\alpha\sin^2\left(\frac{k_2\pi}{2m}\right) + 2\beta\left[1-\cos\left(\frac{k_1\pi}{n}\right)\cos\left(\frac{k_2\pi}{m}\right)\right] + 16\gamma\sin^2\left(\frac{k_1\pi}{2n}\right) - M\omega^2 \end{cases} \tag{11}$$

The vanishing of the determinant of the system in Equation (9) or Equation (10), with the positions in Equation (11), gives a quartic characteristic equation for the in-plane

eigenfrequencies of the rectangular lattice constrained according to cases A or B, which is then:

$$A_{11}\left(\omega^2\right)A_{22}\left(\omega^2\right) - A_{12}A_{21} = 0 \tag{12}$$

This quartic equation can be explicitly written as:

$$\begin{array}{l} M^2\omega^4 \\ -M\omega^2\left[(4\alpha+16\gamma)\left[\sin^2\left(\frac{k_1\pi}{2n}\right)+\sin^2\left(\frac{k_2\pi}{2m}\right)\right]+4\beta\left[1-\cos\left(\frac{k_1\pi}{n}\right)\cos\left(\frac{k_2\pi}{m}\right)\right]\right] \\ +\left[4\alpha\sin^2\left(\frac{k_1\pi}{2n}\right)+2\beta\left[1-\cos\left(\frac{k_1\pi}{n}\right)\cos\left(\frac{k_2\pi}{m}\right)\right]+16\gamma\sin^2\left(\frac{k_2\pi}{2m}\right)\right] \\ \left[4\alpha\sin^2\left(\frac{k_2\pi}{2m}\right)+2\beta\left[1-\cos\left(\frac{k_1\pi}{n}\right)\cos\left(\frac{k_2\pi}{m}\right)\right]+16\gamma\sin^2\left(\frac{k_1\pi}{2n}\right)\right] \\ -(2\beta+4\gamma)^2\sin^2\left(\frac{k_1\pi}{n}\right)\sin^2\left(\frac{k_2\pi}{m}\right)=0 \end{array} \tag{13}$$

and admits two families of solutions: shearing modes (which we will see correspond to smaller roots) and the longitudinal modes (larger roots). For each boundary condition (simply supported edges with case A or B), the modes associated with the eigenfrequencies are selected to preserve the kinematic compatibility, as detailed below for the continuous plate problem.

3. Continuous Calibration and Numerical Results

The difference equations Equation (4) of Gazis et al.'s lattice asymptotically converge to Navier's partial differential equations for a sufficiently small spacing between pairs of particles. Between the discrete and the equivalent continuum connected at the nodal points $u_{i,j} = u(x = ai, y = aj)$ and $v_{i,j} = v(x = ai, y = aj)$, and for sufficiently smooth functions, it is:

$$u_{i+1,j+1} = u(x+a, y+a) = e^{a(\partial_x+\partial_y)}u(x,y) \text{ and } v_{i+1,j+1} = v(x+a, y+a) = e^{a(\partial_x+\partial_y)}v(x,y) \tag{14}$$

We shall make use of the technique developed by Cauchy (1828) [42], which allows the expansion of some difference operators in the Taylor series of differential operators by assuming a sufficiently smooth evolution function. The expansion of the difference operators in the governing equation, Equation (4), up to the first terms yields Navier's type of partial differential equations:

$$\begin{cases} (\alpha+\beta)\frac{\partial^2 u}{\partial x^2} + (2\beta+4\gamma)\frac{\partial^2 v}{\partial x\partial y} + (4\gamma+\beta)\frac{\partial^2 u}{\partial y^2} + \omega^2\frac{M}{a^2}u = 0 \\ (\alpha+\beta)\frac{\partial^2 v}{\partial y^2} + (2\beta+4\gamma)\frac{\partial^2 u}{\partial x\partial y} + (4\gamma+\beta)\frac{\partial^2 v}{\partial x^2} + \omega^2\frac{M}{a^2}v = 0 \end{cases} \tag{15}$$

Navier's asymptotic continuous linear isotropic equations for plane stress are:

$$\begin{cases} \frac{E}{1-v^2}\frac{\partial^2 u}{\partial x^2} + \frac{E}{2(1-v)}\frac{\partial^2 v}{\partial x\partial y} + \frac{E}{2(1+v)}\frac{\partial^2 u}{\partial y^2} + \omega^2\rho u = 0 \\ \frac{E}{1-v^2}\frac{\partial^2 v}{\partial y^2} + \frac{E}{2(1-v)}\frac{\partial^2 u}{\partial x\partial y} + \frac{E}{2(1+v)}\frac{\partial^2 v}{\partial x^2} + \omega^2\rho v = 0 \end{cases} \tag{16}$$

Comparing Equations (15) and (16) makes it possible to identify the elastic constants of the lattice, yielding the following micro/macro scaling relations (see also Challamel et al., 2023 [3]):

$$M = \rho a^2 h \text{ and } \begin{cases} \alpha+\beta = \frac{Eh}{1-v^2} \\ 2\beta+4\gamma = \frac{Eh}{2(1-v)} \\ 4\gamma+\beta = \frac{Eh}{2(1+v)} \end{cases} \Rightarrow \begin{cases} \alpha = \frac{Eh}{1+v} \\ \beta = \frac{Ehv}{1-v^2} \\ \gamma = \frac{Eh(1-3v)}{8(1-v^2)} \end{cases} \tag{17}$$

where h is the depth of the plane element, E the Young's modulus, v is the Poisson's ratio and ρ is the mass density of the material per unit volume.

The definite positivity of the potential energy of Gazis et al.'s lattice in plane stress implies the positivity of each central and non-central stiffness parameters, i.e.,

$$\alpha \geq 0,\ \beta \geq 0 \text{ and } \gamma \geq 0 \ \Rightarrow\ E \geq 0 \text{ and } \upsilon \in \left[0; \frac{1}{3}\right] \tag{18}$$

It is possible to include other non-central interactions, based on the surface potentials, to calibrate the lattice so as to have larger equivalent Poisson's ratios υ, as shown by Challamel et al. (2024) [25].

With these scaling coefficients, the difference equations to be solved for the free vibration of Gazis et al.'s (1960) lattice could be equivalently rewritten as (as obtained by Challamel et al., 2023 [3] or Challamel et al., 2024 [25]):

$$\begin{cases} \frac{E}{1+\upsilon}\left(u_{i+1,j} - 2u_{i,j} + u_{i-1,j}\right) + \frac{E\upsilon}{2(1-\upsilon^2)}\left(u_{i+1,j+1} + u_{i-1,j-1} + u_{i-1,j+1} + u_{i+1,j-1} - 4u_{i,j}\right) + \\ \frac{E}{8(1-\upsilon)}\left(v_{i+1,j+1} - v_{i-1,j+1} - v_{i+1,j-1} + v_{i-1,j-1}\right) + \frac{E(1-3\upsilon)}{2(1-\upsilon^2)}\left(u_{i,j+1} - 2u_{i,j} + u_{i,j-1}\right) + \omega^2\rho a^2\, u_{i,j} = 0 \\ \frac{E}{1+\upsilon}\left(v_{i,j+1} - 2v_{i,j} + v_{i,j-1}\right) + \frac{E\upsilon}{2(1-\upsilon^2)}\left(v_{i+1,j+1} + v_{i-1,j-1} + v_{i-1,j+1} + v_{i+1,j-1} - 4v_{i,j}\right) + \\ \frac{E}{8(1-\upsilon)}\left(u_{i+1,j+1} - u_{i-1,j+1} - u_{i+1,j-1} + u_{i-1,j-1}\right) + \frac{E(1-3\upsilon)}{2(1-\upsilon^2)}\left(v_{i+1,j} - 2v_{i,j} + v_{i-1,j}\right) + \omega^2\rho a^2\, v_{i,j} = 0 \end{cases} \tag{19}$$

In this way, the elastic lattice turns to a finite difference (FD) formulation of the continuous elastic plate (see Challamel et al. [3]). It is also possible to provide a non-dimensional formulation of the problem, starting from the introduction of the dimensionless frequency Ω:

$$\Omega = \frac{\omega\, L_1}{c_L} \text{ with } c_L = \sqrt{\frac{E}{\rho(1-\upsilon^2)}} \tag{20}$$

where c_L is the longitudinal wave speed of the asymptotic elastic linear isotropic continuum. The dimensionless frequency can be also defined with respect to the lattice parameters:

$$\Omega = \frac{\omega\, L_1}{c_L} \text{ with } c_L = \sqrt{\frac{\alpha+\beta}{\rho h}} = a\sqrt{\frac{\alpha+\beta}{M}} \tag{21}$$

By Equations (20) and (21), the difference equations, Equation (19), can be equivalently formulated as:

$$\begin{cases} (1-\upsilon)\left(u_{i+1,j} - 2u_{i,j} + u_{i-1,j}\right) + \frac{\upsilon}{2}\left(u_{i+1,j+1} + u_{i-1,j-1} + u_{i-1,j+1} + u_{i+1,j-1} - 4u_{i,j}\right) + \\ \frac{1+\upsilon}{8}\left(v_{i+1,j+1} - v_{i-1,j+1} - v_{i+1,j-1} + v_{i-1,j-1}\right) + \frac{1-3\upsilon}{2}\left(u_{i,j+1} - 2u_{i,j} + u_{i,j-1}\right) + \frac{\Omega^2}{n^2}\, u_{i,j} = 0 \\ (1-\upsilon)\left(v_{i,j+1} - 2v_{i,j} + v_{i,j-1}\right) + \frac{\upsilon}{2}\left(v_{i+1,j+1} + v_{i-1,j-1} + v_{i-1,j+1} + v_{i+1,j-1} - 4v_{i,j}\right) + \\ \frac{1+\upsilon}{8}\left(u_{i+1,j+1} - u_{i-1,j+1} - u_{i+1,j-1} + u_{i-1,j-1}\right) + \frac{1-3\upsilon}{2}\left(v_{i+1,j} - 2v_{i,j} + v_{i-1,j}\right) + \frac{\Omega^2}{n^2}\, v_{i,j} = 0 \end{cases} \tag{22}$$

The discrete eigenfrequency problem only depends on three dimensionless parameters, Poisson's ratio υ and the number of particles in each direction n and m:

$$\Omega = \Omega(\upsilon, n, m) \tag{23}$$

For a square plate, the eigenfrequency problem only depends on the Poisson's ratio and the number $n = m$ of particles, $\Omega = \Omega(\upsilon, n)$. At the asymptotic limit $n \to \infty$, i.e., for the asymptotic continuum, the eigenfrequency determination of the square continuous plate only depends on the Poisson's ratio υ.

The numerical results for the in-plane eigenfrequencies of square lattices composed of 10×10, 20×20 and 40×40 Gazis et al.'s cells with the Poisson's ratio $\upsilon = 0.3$ are presented in Tables 1 and 2 (case A), and in Tables 3 and 4 (case B). Tables 1 and 3 show a perfect agreement between the analytical solution obtained from the quartic equation and the direct numerical method based on matrix eigenvalues. The eigenfrequencies increase with respect to the number n of cells, and asymptotically converge to those of the continuous plate. It is also confirmed that the two cases, A and B, controlled by the same eigenfrequency

equation, do not have the same spectra, due to the incompatibility of some modes with the given constraints. Consequently, the two boundary conditions yield distinct spectra for both the lattice and the asymptotic continuum. The eigenmode numbers associated with each mode are indicated in Tables 2 and 4 for cases A and B, respectively. The eigenmodes for both boundary conditions are shown in Figures 5 and 6: note that the mode shapes of both the lattice and continuum do not depend on the Poisson's ratio, as highlighted by the eigenmode equations, Equation (7) (case A) and Equation (8) (case B). The 10 first modes are shown for cases A and B for the 20 × 20 cells lattice: this confirms the physical difference between the two lattices with distinct constraints. The lattice appears well suited for a better understanding of the discrete modes according to the lattice cell deformations.

Table 1. Comparison of eigenfrequencies Ω between the lattice solution (analytical) and the numerical lattice solution from the algebraic eigenvalue computation—υ = 0.3—case A.

Mode	Numerical Solutions for Lattice Model, Ω			Analytical Solutions for Lattice Model, Ω			Analytical Solutions for Continuous Plate, Ω
	10 × 10 Cell Lattice	20 × 20 Cell Lattice	40 × 40 Cell Lattice	10 × 10 Cell Lattice	20 × 20 Cell Lattice	40 × 40 Cell Lattice	
1	1.851	1.857	1.858	1.851	1.857	1.858	1.859
2	1.851	1.857	1.858	1.851	1.857	1.858	1.859
3	2.620	2.626	2.628	2.620	2.626	2.628	2.628
4	3.656	3.702	3.713	3.656	3.702	3.713	3.717
5	3.656	3.702	3.713	3.656	3.702	3.713	3.717
6	4.104	4.143	4.153	4.104	4.143	4.153	4.156
7	4.104	4.143	4.153	4.104	4.143	4.153	4.156
8	4.391	4.430	4.440	4.391	4.430	4.440	4.443
9	5.188	5.240	5.253	5.188	5.240	5.253	5.257
10	5.372	5.524	5.563	5.372	5.524	5.563	5.576

Table 2. Eigenfrequency Ω and eigenmode lattice solution (numerical and analytical)—υ = 0.3—case A.

Mode	Eigenmode Numbers and Mode Type			Analytical and Numerical Solutions for Lattice Model, Ω			Analytical Solutions for Continuous Plate, Ω
	k_1	k_2	Mode	10 × 10 Cell Lattice	20 × 20 Cell Lattice	40 × 40 Cell Lattice	
1	0	1	shearing	1.851	1.857	1.858	1.859
2	1	0	shearing	1.851	1.857	1.858	1.859
3	1	1	shearing	2.620	2.626	2.628	2.628
4	0	2	shearing	3.656	3.702	3.713	3.717
5	2	0	shearing	3.656	3.702	3.713	3.717
6	1	2	shearing	4.104	4.143	4.153	4.156
7	2	1	shearing	4.104	4.143	4.153	4.156
8	1	1	longitudinal	4.391	4.430	4.440	4.443
9	2	2	shearing	5.188	5.240	5.253	5.257
10	0	3	shearing	5.372	5.524	5.563	5.576

Table 3. Comparison of eigenfrequencies Ω between the lattice solution (analytical) and the numerical lattice solution from the algebraic eigenvalue computation—υ = 0.3—case B.

Mode	Numerical Solutions for Lattice Model, Ω			Analytical Solutions for Lattice Model, Ω			Analytical Solutions for Continuous Plate, Ω
	10 × 10 Cell Lattice	20 × 20 Cell Lattice	40 × 40 Cell Lattice	10 × 10 Cell Lattice	20 × 20 Cell Lattice	40 × 40 Cell Lattice	
1	2.620	2.626	2.628	2.620	2.626	2.628	2.628
2	3.129	3.138	3.141	3.129	3.138	3.141	3.142
3	3.129	3.138	3.141	3.129	3.138	3.141	3.142
4	4.104	4.143	4.153	4.104	4.143	4.153	4.156
5	4.104	4.143	4.153	4.104	4.143	4.153	4.156
6	4.391	4.430	4.440	4.391	4.430	4.440	4.443
7	5.188	5.240	5.253	5.188	5.240	5.253	5.257
8	5.691	5.830	5.866	5.691	5.830	5.866	5.877
9	5.691	5.830	5.866	5.691	5.830	5.866	5.877
10	6.180	6.257	6.277	6.180	6.257	6.277	6.283

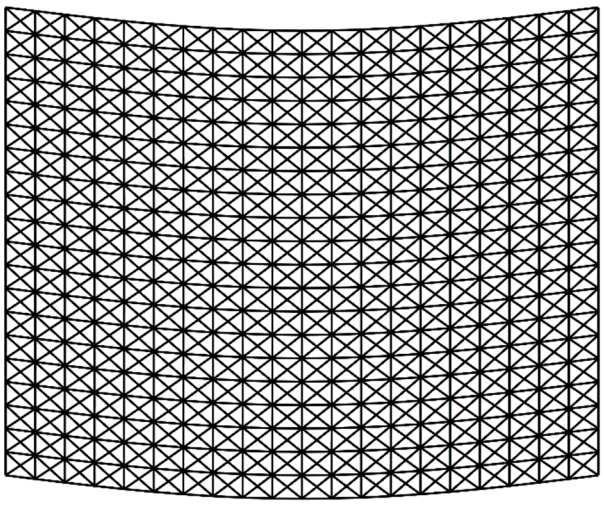

Mode 1

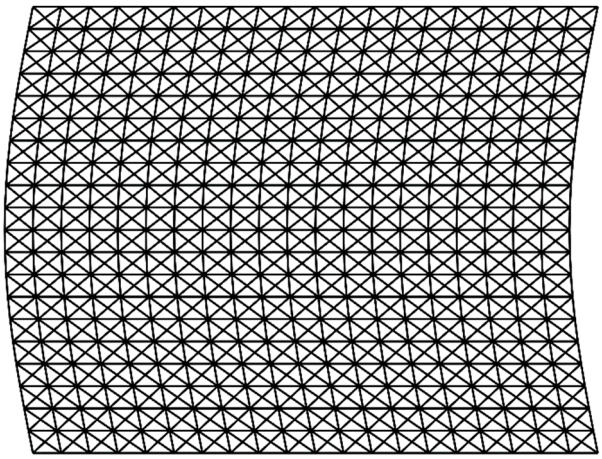

Mode 2

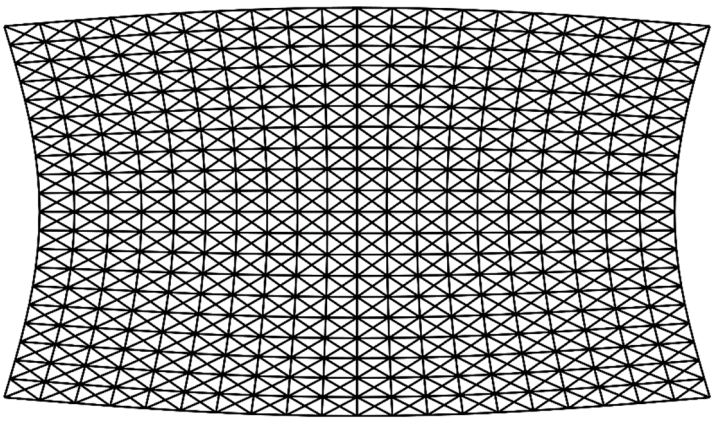

Mode 3

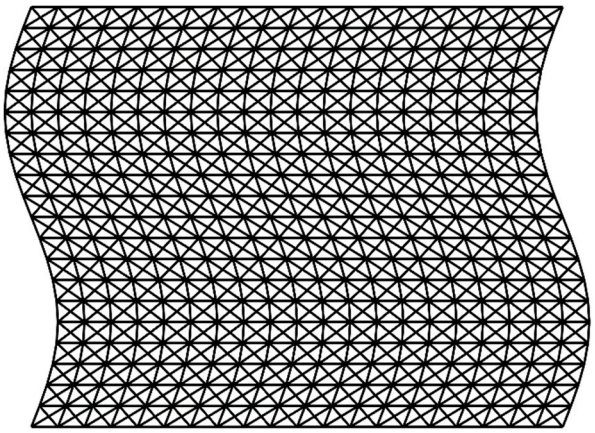

Mode 4

Figure 5. *Cont*.

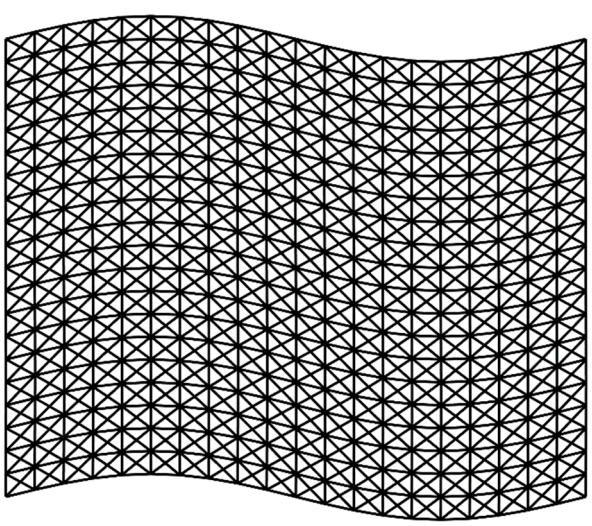

Mode 5

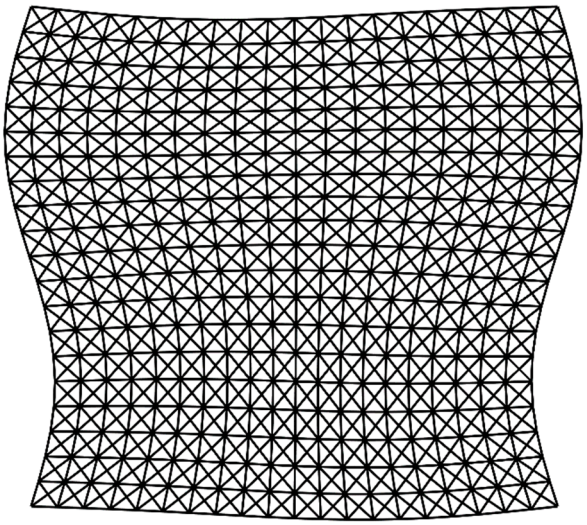

Mode 6

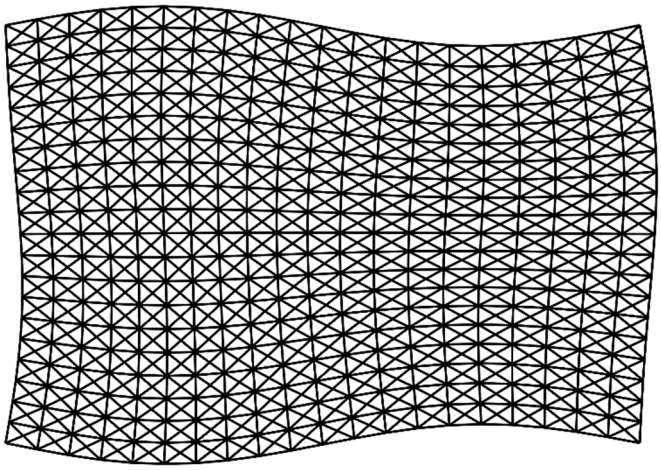

Mode 7

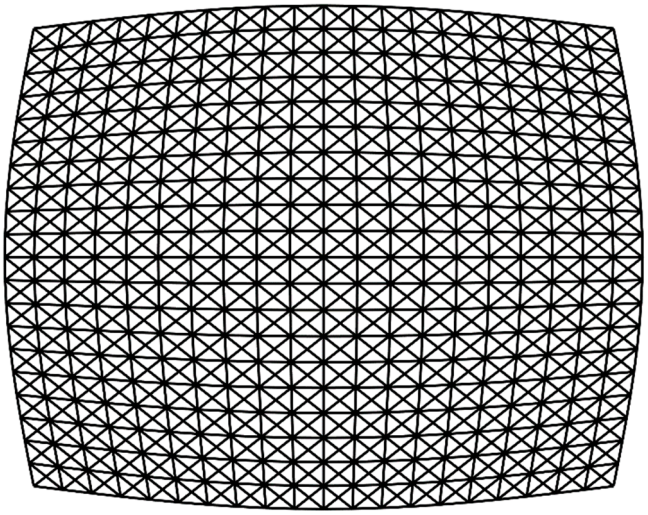

Mode 8

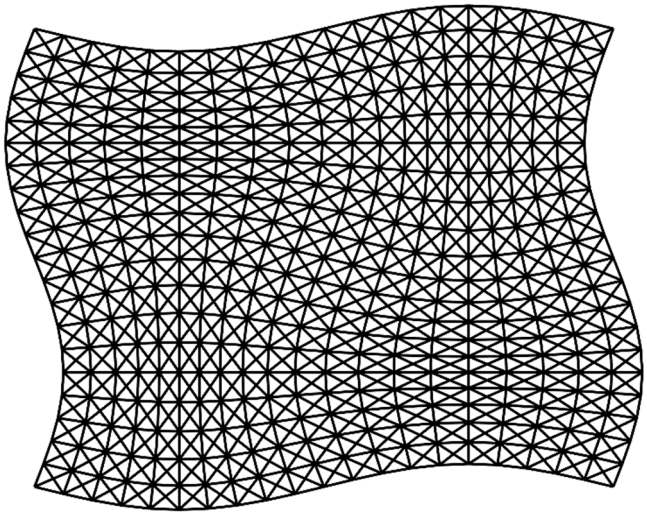

Mode 9

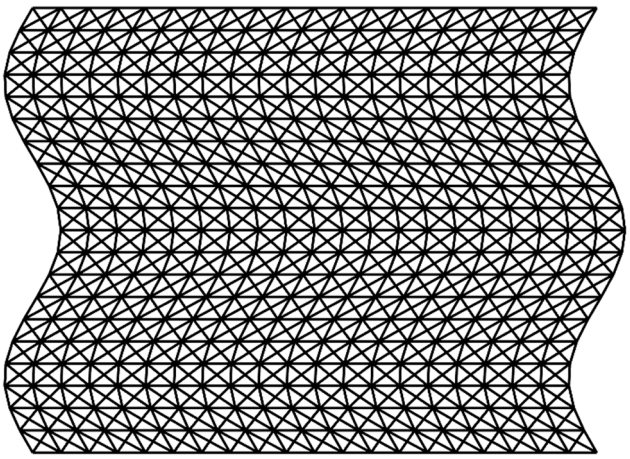

Mode 10

Figure 5. Eigenmodes of the lattice plate on sliding support (for the in-plane lattice plate problem)—20 × 20 cell square lattice (case A).

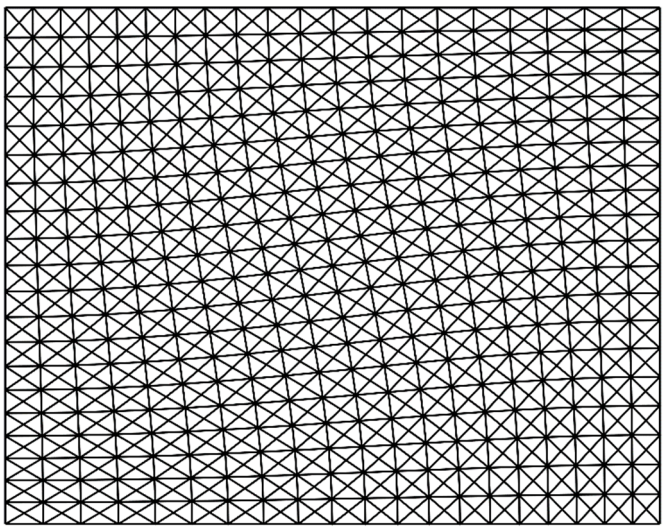

Mode 1

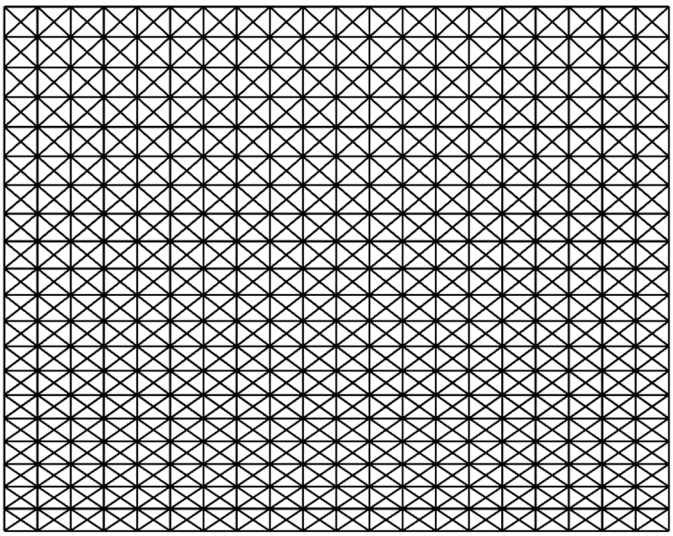

Mode 2

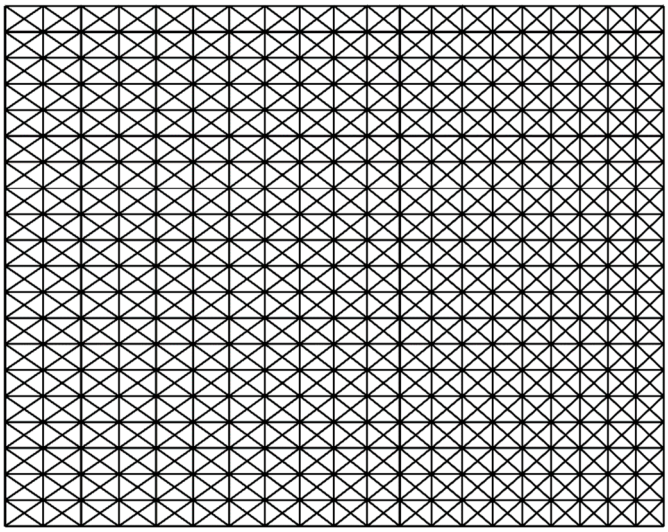

Mode 3

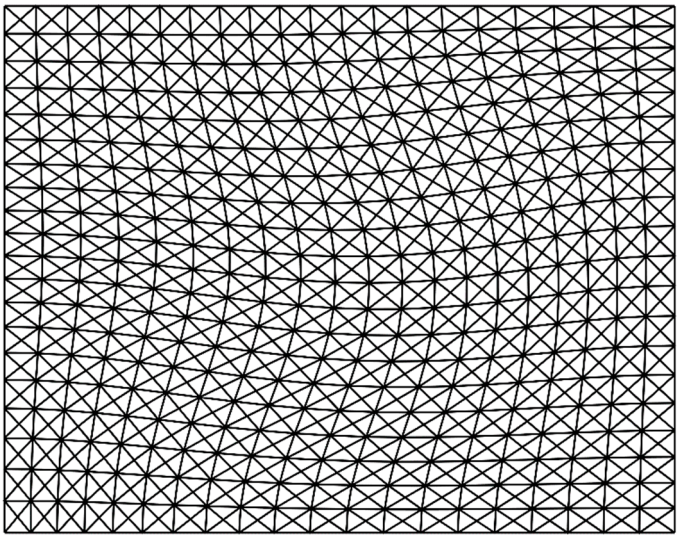

Mode 4

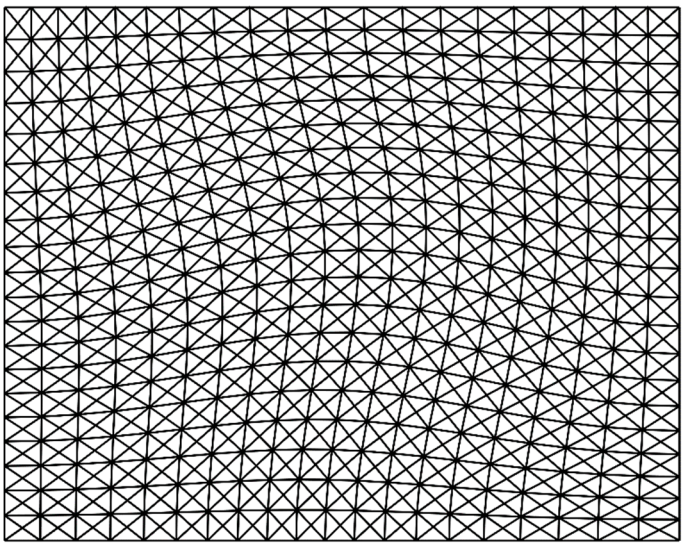

Mode 5

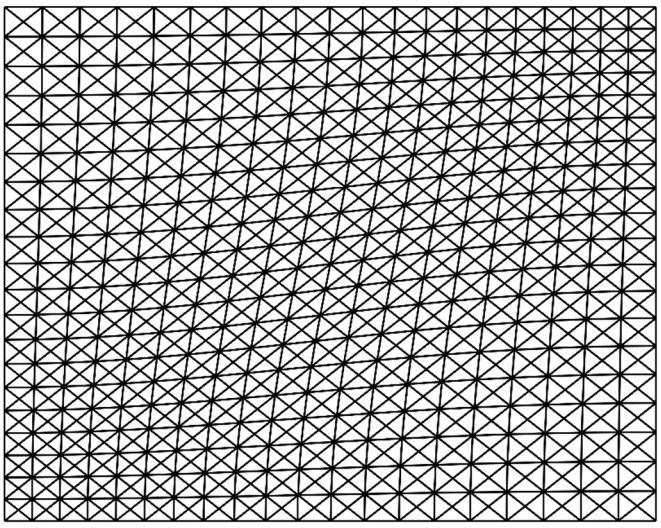

Mode 6

Figure 6. *Cont*.

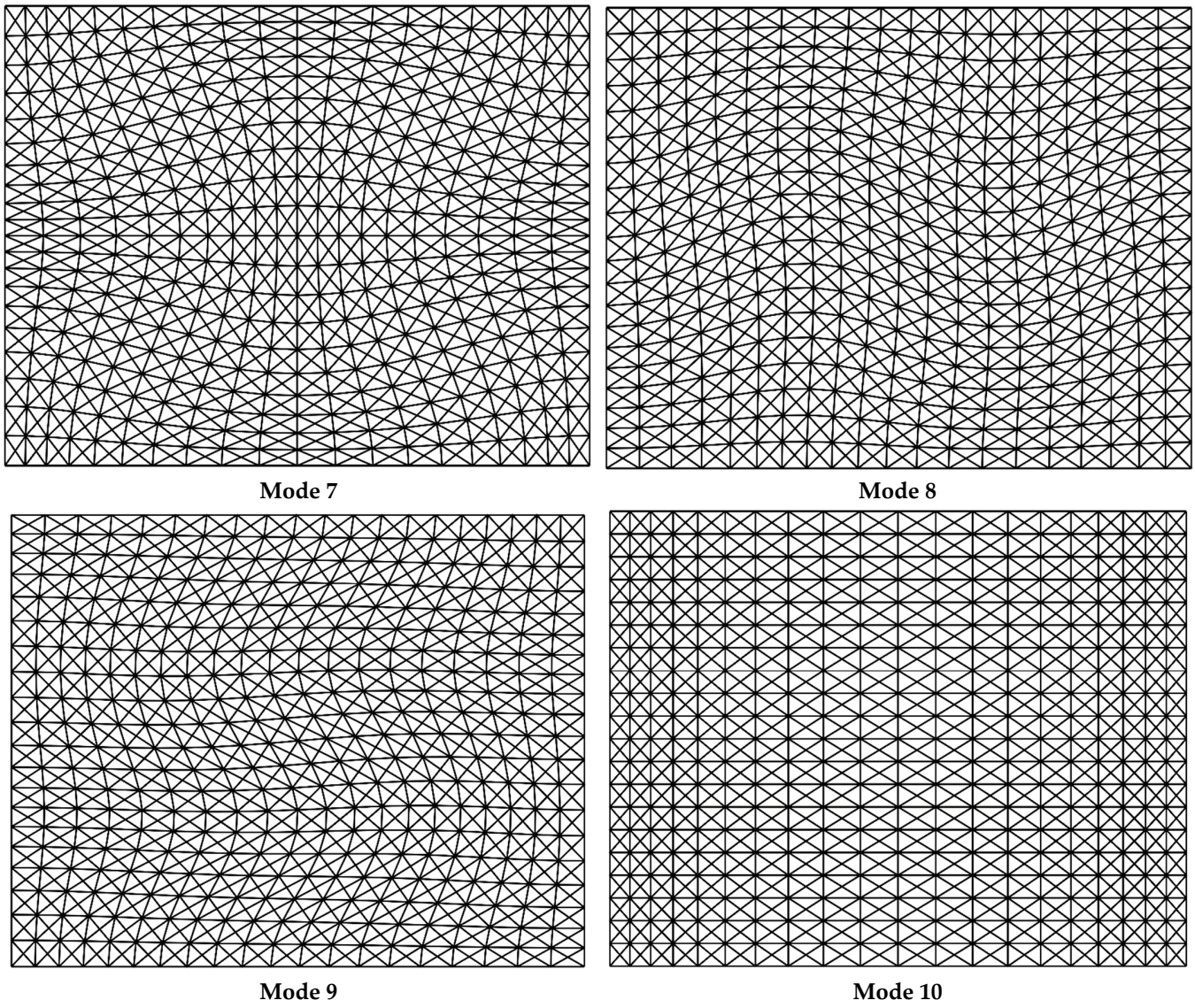

Figure 6. Eigenmodes of the lattice plate on sliding support (for the in-plane lattice plate problem)—20 × 20 cell square lattice (case B).

Table 4. Eigenfrequency Ω and eigenmode lattice solution (numerical and analytical)—υ = 0.3—case B.

Mode	Eigenmode Numbers and Mode Type			Analytical Solutions for Lattice Model, Ω			Analytical Solutions for Continuous Plate, Ω
	k_1	k_2	Mode	10 × 10 Cell Lattice	20 × 20 Cell Lattice	40 × 40 Cell Lattice	
1	1	1	shearing	2.620	2.626	2.628	2.628
2	0	1	longitudinal	3.129	3.138	3.141	3.142
3	1	0	longitudinal	3.129	3.138	3.141	3.142
4	1	2	shearing	4.104	4.143	4.153	4.156
5	2	1	shearing	4.104	4.143	4.153	4.156

Table 4. *Cont.*

Mode	Eigenmode Numbers and Mode Type			Analytical Solutions for Lattice Model, Ω			Analytical Solutions for Continuous Plate, Ω
	k_1	k_2	Mode	10 × 10 Cell Lattice	20 × 20 Cell Lattice	40 × 40 Cell Lattice	
6	1	1	longitudinal	4.391	4.430	4.440	4.443
7	2	2	shearing	5.188	5.240	5.253	5.257
8	1	3	shearing	5.691	5.830	5.866	5.877
9	3	1	shearing	5.691	5.830	5.866	5.877
10	0	2	longitudinal	6.180	6.257	6.277	6.283

4. In-Plane Vibrations of Continuous Plates—Rayleigh Solution

We now detail and comment on the exact solution of continuous plates compared to that of discrete lattices. Navier's partial differential equations for linear isotropic elastic plates, Equation (16), hold for plane stress and describe the in-plane vibration. As for the lattice constrained by sliding supports, we consider two boundary conditions (see also Gorman, 2006 [38]):

- In case A (Figure 2), the continuous tangential displacement and normal stress vanish (sliding supports normal to the boundary). The solution can be thought of in the same form considered for the lattice under the constraints of case A:

$$u(x,y) = U\cos\left(\frac{k_1\pi\,x}{L_1}\right)\sin\left(\frac{k_2\pi\,y}{L_2}\right) \text{ and } v(x,y) = V\sin\left(\frac{k_1\pi\,x}{L_1}\right)\cos\left(\frac{k_2\pi\,y}{L_2}\right) \tag{24}$$

- In case B (Figure 4), the continuous normal displacement and shear stress vanish (sliding supports along the boundary). The solution can be thought of in the same form considered for the lattice under the constraints of case B:

$$u(x,y) = U\sin\left(\frac{k_1\pi\,x}{L_1}\right)\cos\left(\frac{k_2\pi\,y}{L_2}\right) \text{ and } v(x,y) = V\cos\left(\frac{k_1\pi\,x}{L_1}\right)\sin\left(\frac{k_2\pi\,y}{L_2}\right) \tag{25}$$

The substitution of Equation (24) into Equation (16), or Equation (25) into Equation (16) gives the same eigenfrequency solution (for both simply supported boundary conditions) for the linear elastic 2D continuous medium in plane stress, which coincides with the expressions in Rayleigh (1894) [35]:

$$\begin{cases} \left[\frac{E}{1-v^2}\left(\frac{k_1\pi}{L_1}\right)^2+\frac{E}{2(1+v)}\left(\frac{k_2\pi}{L_2}\right)^2-\rho\omega^2\right]U+\frac{E}{2(1-v)}\left(\frac{k_1\pi}{L_1}\right)\left(\frac{k_2\pi}{L_2}\right)V=0 \\ \frac{E}{2(1-v)}\left(\frac{k_1\pi}{L_1}\right)\left(\frac{k_2\pi}{L_2}\right)U+\left[\frac{E}{1-v^2}\left(\frac{k_2\pi}{L_2}\right)^2+\frac{E}{2(1+v)}\left(\frac{k_1\pi}{L_1}\right)^2-\rho\omega^2\right]V=0 \end{cases} \tag{26}$$

From Equation (26), the eigenfrequencies are solutions of a quartic equation:

$$\begin{aligned} &\left[\frac{E}{1-v^2}\left(\frac{k_1\pi}{L_1}\right)^2+\frac{E}{2(1+v)}\left(\frac{k_2\pi}{L_2}\right)^2-\rho\omega^2\right]\left[\frac{E}{1-v^2}\left(\frac{k_2\pi}{L_2}\right)^2+\frac{E}{2(1+v)}\left(\frac{k_1\pi}{L_1}\right)^2-\rho\omega^2\right] \\ &-\frac{E^2}{4(1-v)^2}\left(\frac{k_1\pi}{L_1}\right)^2\left(\frac{k_2\pi}{L_2}\right)^2=0 \end{aligned} \tag{27}$$

which may be presented in the equivalent form:

$$\left(\rho\omega^2\right)^2-\frac{E(3-v)}{2(1-v^2)}\left[\left(\frac{k_1\pi}{L_1}\right)^2+\left(\frac{k_2\pi}{L_2}\right)^2\right]\rho\omega^2+\frac{E^2}{2(1+v)(1-v^2)}\left[\left(\frac{k_1\pi}{L_1}\right)^2+\left(\frac{k_2\pi}{L_2}\right)^2\right]^2=0 \tag{28}$$

Equation (28) gives the two families of frequencies for the in-plane vibration in plane stress:

$$\rho\omega^2 = \frac{1}{4}\frac{E}{1-v^2}[3-v\pm(1+v)]\left[\left(\frac{k_1\pi}{L_1}\right)^2+\left(\frac{k_2\pi}{L_2}\right)^2\right] \tag{29}$$

The position in Equation (20) holds here also; thus, we obtain the non-dimensional frequency of the continuous plate for both boundary conditions:

$$\Omega^2 = \frac{1}{4}[3-v\pm(1+v)]\pi^2\left[k_1^2+k_2^2\left(\frac{L_1}{L_2}\right)^2\right] \tag{30}$$

which can be also written as:

$$\Omega^2 = \frac{1-v}{2}\pi^2\left[k_1^2+k_2^2\left(\frac{L_1}{L_2}\right)^2\right] \text{ for the shearing modes}$$

$$\text{or } \Omega^2 = \pi^2\left[k_1^2+k_2^2\left(\frac{L_1}{L_2}\right)^2\right] \text{ for the longitudinal modes} \tag{31}$$

Equation (31) was obtained by Rayleigh (page 405 of Rayleigh, 1894 [35]) and numerically confirmed by Bardell et al. (1996) [37] using a Rayleigh–Ritz approach. Rayleigh (1894) [35] implicitly gave the solution for a cylinder with an infinite radius that converges to a plate, with cyclic boundary conditions equivalent to simple supports.

For a square plate, $L_1 = L_2$, and we have for both boundary conditions:

$$\Omega = \sqrt{\frac{1-v}{2}}\pi\sqrt{k_1^2+k_2^2} \text{ for the shearing modes}$$

$$\text{or } \Omega = \pi\sqrt{k_1^2+k_2^2} \text{ for the longitudinal modes} \tag{32}$$

It is worth studying the situations when k_1 or k_2 vanishes; for instance, let $k_2 = 0$ in Equation (26):

$$\begin{cases} \left[\frac{E}{1-v^2}\left(\frac{k_1\pi}{L_1}\right)^2-\rho\omega^2\right]U = 0 \\ \left[\frac{E}{2(1+v)}\left(\frac{k_1\pi}{L_1}\right)^2-\rho\omega^2\right]V = 0 \end{cases} \tag{33}$$

For the boundary condition of free normal stress (case A), $k_2 = 0$ is associated with $U = 0$; then, only the shearing modes must be considered:

$$k_2 = 0 \;\Rightarrow\; \Omega = k_1\pi\sqrt{\frac{1-v}{2}} \tag{34}$$

An analogous result is obtained considering $k_1 = 0$; thus, for $k_1 = 0$ or $k_2 = 0$ and the boundary conditions of case A, only the shearing modes must be selected:

$$k_1 = 0 \;\Rightarrow\; \Omega = k_2\pi\sqrt{\frac{1-v}{2}} \text{ or } k_2 = 0 \;\Rightarrow\; \Omega = k_1\pi\sqrt{\frac{1-v}{2}} \tag{35}$$

For the boundary condition of no normal displacement (case B), $k_2 = 0$ is associated with $V = 0$; then, only the longitudinal modes must be considered:

$$k_2 = 0 \;\Rightarrow\; \Omega = k_1\pi \tag{36}$$

An analogous result is obtained considering $k_1 = 0$; thus, for $k_1 = 0$ or $k_2 = 0$ and the boundary conditions of case B, only the longitudinal modes must be selected:

$$k_1 = 0 \Rightarrow \Omega = k_2\pi \text{ or } k_2 = 0 \Rightarrow \Omega = k_1\pi \tag{37}$$

To summarise, the two boundary conditions of cases A and B are associated with the same spectrum (with different mode shapes), except for the limit situation in which $k_1k_2 = 0$. In such situation, we must consider only pure shear modes for case A and only pure longitudinal modes for case B. The numerical results are presented in Table 5 for a continuous square plate constrained as in cases A and B.

Table 5. Exact eigenfrequencies Ω of a simply supported square local continuous plate—in-plane vibrations; case A and case B boundary conditions; υ = 0.3.

(k_1, k_2)	Case A (as Analysed by Bardell et al., 1996 [37])	Case B
(0, 1)	π[(1 − υ)/2]^0.5 ≈ 1.859	
(1, 0)	π[(1 − υ)/2]^0.5 ≈ 1.859	
(1, 1)	π[1 − υ]^0.5 ≈ 2.628	π[1 − υ]^0.5 ≈ 2.628
(0, 1) †		π ≈ 3.142
(1, 0) †		π ≈ 3.142
(0, 2)	π[2*(1 − υ)]^0.5 ≈ 3.717	
(2, 0)	π[2*(1 − υ)]^0.5 ≈ 3.717	
(1, 2)	π[5*(1 − υ)/2]^0.5 ≈ 4.156	π[5*(1 − υ)/2]^0.5 ≈ 4.156
(2, 1)	π[5*(1 − υ)/2]^0.5 ≈ 4.156	π[5*(1 − υ)/2]^0.5 ≈ 4.156
(1, 1) †	π[2]^0.5 ≈ 4.443	π[2]^0.5 ≈ 4.443
(2, 2)	2π[1 − υ]^0.5 ≈ 5.257	2π[1 − υ]^0.5 ≈ 5.257

† These are longitudinal modes (all the others are shearing modes).

In conclusion, the eigenfrequencies for the square plate constrained as in case A are:

$$\Omega = \sqrt{\frac{1-v}{2}}\pi\sqrt{k_1^2 + k_2^2} \text{ for the shearing modes including } k_1k_2 = 0$$

$$\text{or } \Omega = \pi\sqrt{k_1^2 + k_2^2} \text{ for the longitudinal modes with } k_1k_2 \neq 0 \tag{38}$$

The eigenfrequencies for the square plate constrained as in case B are:

$$\Omega = \sqrt{\frac{1-v}{2}}\pi\sqrt{k_1^2 + k_2^2} \text{ for the shearing modes with } k_1k_2 \neq 0$$

$$\text{or } \Omega = \pi\sqrt{k_1^2 + k_2^2} \text{ for the longitudinal modes including } k_1k_2 = 0 \tag{39}$$

The same conclusions hold for the plane lattice for both boundary conditions of cases A and B. Note that the modes of the lattice and of the continuous plate coincide, while the eigenfrequencies differ between the discrete and the continuous problem. As highlighted by Tables 1 and 3, the eigenfrequencies of the plane lattice converge to those of the continuous plate from below, as classically obtained from Finite Difference Methods (FDMs) applied to homogeneous structural dynamic problems (see, for instance, Collatz, 1960 [43]; Challamel et al., 2015 [44]; Wang et al., 2020 [6]). Challamel et al. (2015) [44] commented on the lower status of FDM for one-dimensional continuous eigenvalue problems, such as the free vibration of finite rods or strings. The FDM has also a lower bound status for the eigenfrequency calculation of continuous membranes with the so-called lumped mass

method (see also Polya, 1952 [45] or Tong et al., 1971 [14] for FD linear 2D homogeneous eigenvalue problems such as that of the membrane). It is worth mentioning that the lower bound or upper bound status of the discrete approach is strongly sensitive to the mass repartition in the lattice, as analysed by Polya (1952) [45] for the discrete membrane problem or Challamel et al. (2016) [46] for the discrete rod or string problem (lumped mass method as opposed to the consistent distributed mass method).

5. Higher-Order Elasticity and Nonlocal Elasticity

By using the continualisation procedure presented in Equation (14), the difference eigenvalue problem in Equation (22) can be approximated via a higher-order elasticity continuous eigenvalue problem, by considering second-order terms in the asymptotic expansion of the difference operators:

$$\begin{cases} \frac{\partial^2 u}{\partial x^2} + \left(\frac{1+v}{2}\right)\frac{\partial^2 v}{\partial x \partial y} + \left(\frac{1-v}{2}\right)\frac{\partial^2 u}{\partial y^2} \\ + \frac{a^2}{12}\left[\frac{\partial^4 u}{\partial x^4} + \left(\frac{1-v}{2}\right)\frac{\partial^4 u}{\partial y^4} + 6v\frac{\partial^4 u}{\partial x^2 \partial y^2} + (1+v)\left(\frac{\partial^4 v}{\partial x^3 \partial y} + \frac{\partial^4 v}{\partial x \partial y^3}\right)\right] + \frac{\Omega^2}{L_1^2}u = 0 \\ \frac{\partial^2 v}{\partial y^2} + \left(\frac{1+v}{2}\right)\frac{\partial^2 u}{\partial x \partial y} + \left(\frac{1-v}{2}\right)\frac{\partial^2 v}{\partial x^2} \\ + \frac{a^2}{12}\left[\frac{\partial^4 v}{\partial y^4} + \left(\frac{1-v}{2}\right)\frac{\partial^4 v}{\partial x^4} + 6v\frac{\partial^4 v}{\partial x^2 \partial y^2} + (1+v)\left(\frac{\partial^4 u}{\partial x^3 \partial y} + \frac{\partial^4 u}{\partial x \partial y^3}\right)\right] + \frac{\Omega^2}{L_1^2}v = 0 \end{cases} \tag{40}$$

Mindlin (1968) [26] adopted the same reasoning to derive cubic strain gradient elasticity equations from the 3D lattice model of Gazis et al. [20]. Equation (40) corresponds to the partial differential equations of a strain gradient elastic continuum under plane stress assumptions, with additional terms proportional to $a^2/12$ that account for the lattice's small-scale effects. Equation (40) was also derived by Challamel et al. (2023) [3] and Challamel et al. (2024) [25].

The substitution of Equation (24) into Equation (40) or Equation (25) into Equation (40) gives the same linear system (for both simply supported boundary conditions) for the linear strain gradient elastic 2D medium:

$$\begin{cases} B_{11}(\Omega^2)\, U + B_{12} V = 0 \\ B_{21} U + B_{22}(\Omega^2)\, V = 0 \end{cases} \tag{41}$$

with:

$$\begin{cases} B_{11}(\Omega^2) = \left(\frac{k_1\pi}{L_1}\right)^2\left[1 - \frac{a^2}{12}\left(\frac{k_1\pi}{L_1}\right)^2\right] \\ + \left(\frac{1-v}{2}\right)\left(\frac{k_2\pi}{L_2}\right)^2\left[1 - \frac{a^2}{12}\left(\frac{k_2\pi}{L_2}\right)^2\right] - \frac{a^2}{2}v\left(\frac{k_1\pi}{L_1}\right)^2\left(\frac{k_2\pi}{L_2}\right)^2 - \frac{\Omega^2}{L_1^2} \\ B_{21} = B_{12} = \left(\frac{1+v}{2}\right)\left(\frac{k_1\pi}{L_1}\right)\left(\frac{k_2\pi}{L_2}\right) - \frac{a^2}{12}(1+v)\left(\frac{k_1\pi}{L_1}\right)\left(\frac{k_2\pi}{L_2}\right)\left[\left(\frac{k_1\pi}{L_1}\right)^2 + \left(\frac{k_2\pi}{L_2}\right)^2\right] \\ B_{22}(\Omega^2) = \left(\frac{k_2\pi}{L_2}\right)^2\left[1 - \frac{a^2}{12}\left(\frac{k_2\pi}{L_2}\right)^2\right] \\ + \left(\frac{1-v}{2}\right)\left(\frac{k_1\pi}{L_1}\right)^2\left[1 - \frac{a^2}{12}\left(\frac{k_1\pi}{L_1}\right)^2\right] - \frac{a^2}{2}v\left(\frac{k_1\pi}{L_1}\right)^2\left(\frac{k_2\pi}{L_2}\right)^2 - \frac{\Omega^2}{L_1^2} \end{cases} \tag{42}$$

The quartic equation for the in-plane eigenfrequencies of the lattice-based rectangular strain gradient elastic plate (with case A or case B boundary conditions) is then obtained from:

$$B_{11}\left(\Omega^2\right) B_{22}\left(\Omega^2\right) - B_{12}B_{21} = 0 \tag{43}$$

A nonlocal plate model is obtained by multiplying the partial differential equations, Equation (40), by the differential operator $(1 - a^2\Delta/12)$, where Δ is the 2D Laplacian operator, and limiting to the terms in a^2 to avoid higher-order differential operators (see also Challamel et al., 2022 [39] who applied this methodology for deriving 2D lattice-based

nonlocal elasticity equations in plane strain, or Zhang et al., 2021 [47] for alternative 2D lattices in plane stress). The nonlocal elasticity equations in plane stress are:

$$\begin{cases} \frac{\partial^2 u}{\partial x^2} + \left(\frac{1+\upsilon}{2}\right)\frac{\partial^2 v}{\partial x \partial y} + \left(\frac{1-\upsilon}{2}\right)\frac{\partial^2 u}{\partial y^2} \\ + \frac{a^2}{24}\left[(-3+13\upsilon)\frac{\partial^4 u}{\partial x^2 \partial y^2} + (1+\upsilon)\left(\frac{\partial^4 v}{\partial x^3 \partial y} + \frac{\partial^4 v}{\partial x \partial y^3}\right)\right] + \frac{\Omega^2}{L_1^2}\left(1 - \frac{a^2}{12}\Delta\right)u = 0 \\ \frac{\partial^2 v}{\partial y^2} + \left(\frac{1+\upsilon}{2}\right)\frac{\partial^2 u}{\partial x \partial y} + \left(\frac{1-\upsilon}{2}\right)\frac{\partial^2 v}{\partial x^2} \\ + \frac{a^2}{24}\left[(-3+13\upsilon)\frac{\partial^4 v}{\partial x^2 \partial y^2} + (1+\upsilon)\left(\frac{\partial^4 u}{\partial x^3 \partial y} + \frac{\partial^4 u}{\partial x \partial y^3}\right)\right] + \frac{\Omega^2}{L_1^2}\left(1 - \frac{a^2}{12}\Delta\right)v = 0 \end{cases} \tag{44}$$

This lattice-based nonlocal plate model has the advantage of avoiding higher-order differential operators and the discussion of higher-order variationally based boundary conditions. As already commented by Zhang et al. (2021) [47] or Challamel et al. (2022) [39], these lattice-based partial differential equations differ from the in-plane Eringen's nonlocal plate model (based on Eringen's differential law—Eringen, 1983 [48] applied to plate mechanics), due to the additional spatial coupling terms in Equation (44) (this phenomenon was already commented on for the out-of-plane responses of lattice plates in Challamel et al., 2021 [18]). The substitution of Equation (24) into Equation (44), or Equation (25) into Equation (44) gives the same linear system (for both simply supported boundary conditions) for the linear lattice-based nonlocal elastic 2D medium:

$$\begin{cases} C_{11}(\Omega^2)\, U + C_{12} V = 0 \\ C_{21} U + C_{22}(\Omega^2)\, V = 0 \end{cases} \tag{45}$$

with:

$$\begin{cases} C_{11}(\Omega^2) = \left(\frac{k_1\pi}{L_1}\right)^2 + \left(\frac{1-\upsilon}{2}\right)\left(\frac{k_2\pi}{L_2}\right)^2 - \frac{a^2}{24}(-3+13\upsilon)\left(\frac{k_1\pi}{L_1}\right)^2\left(\frac{k_2\pi}{L_2}\right)^2 \\ \quad - \frac{\Omega^2}{L_1^2}\left[1 + \frac{a^2}{12}\left[\left(\frac{k_1\pi}{L_1}\right)^2 + \left(\frac{k_2\pi}{L_2}\right)^2\right]\right] \\ C_{21} = C_{12} = \left(\frac{1+\upsilon}{2}\right)\left(\frac{k_1\pi}{L_1}\right)\left(\frac{k_2\pi}{L_2}\right)\left[1 - \frac{a^2}{12}\left[\left(\frac{k_1\pi}{L_1}\right)^2 + \left(\frac{k_2\pi}{L_2}\right)^2\right]\right] \\ C_{22}(\Omega^2) = \left(\frac{k_2\pi}{L_2}\right)^2 + \left(\frac{1-\upsilon}{2}\right)\left(\frac{k_1\pi}{L_1}\right)^2 - \frac{a^2}{24}(-3+13\upsilon)\left(\frac{k_1\pi}{L_1}\right)^2\left(\frac{k_2\pi}{L_2}\right)^2 \\ \quad - \frac{\Omega^2}{L_1^2}\left[1 + \frac{a^2}{12}\left[\left(\frac{k_1\pi}{L_1}\right)^2 + \left(\frac{k_2\pi}{L_2}\right)^2\right]\right] \end{cases} \tag{46}$$

The quartic equation for the in-plane eigenfrequencies of the simply supported lattice-based rectangular nonlocal elastic plate (with case A or case B boundary conditions), is then obtained from:

$$C_{11}\left(\Omega^2\right)C_{22}\left(\Omega^2\right) - C_{12}C_{21} = 0 \tag{47}$$

The lattice-based gradient elasticity and the nonlocal elasticity solutions for the plate are then compared to the exact lattice plate solution in Tables 6 and 7 for a 10×10 cell square lattice (with an asymptotic Poisson's ratio υ equal to 0.3), for both boundary conditions. As expected, an excellent agreement can be noticed between the second-order (gradient or nonlocal) elastic plate models and the lattice one, especially for the lower modes. For both models (gradient and nonlocal plate models), and for both simply supported boundary conditions, the fundamental eigenfrequencies of the enriched continuous models coincide with the lattice fundamental eigenfrequencies up to three digits. The difference tends to increase with the mode numbers. This is also confirmed by the curves in Figures 7–9 also valid for the n × n cell square lattice with the asymptotic Poisson's ratio υ equal to 0.3. The dependence of the dimensionless fundamental frequency $\Omega_{1,0} = \Omega_{0,1}$ with respect to the number n of cells in each direction (with case A simply supported boundary conditions) is compared in Figure 7 for the lattice, the strain gradient and the nonlocal elastic plate models. For the three models, the convergence towards the local solution (Rayleigh solution) is from below. Additionally, it is shown that both the gradient elasticity

and the nonlocal elasticity solutions give accurate results for small values of n such as $n = 4$. As expected, the higher-order solutions which are obtained from asymptotic analysis for sufficiently large values of n become more precise with an increasing value of n. The same tendencies are observed in Figure 8 for the dimensionless fundamental frequency $\Omega_{1,1}$ with respect to the number n of cells in each direction (with case B simply supported boundary conditions). For both fundamental eigenfrequencies, the gradient elasticity model furnishes slightly better results than the nonlocal elastic plate model. Finally, the dimensionless eigenfrequency $\Omega_{2,2}$ for both sliding supports—case A (which corresponds to mode 9) or Case B (which corresponds to mode 7) (for the in-plane lattice plate problem)—is plotted versus the number n of cells. The higher-order solutions are less accurate for this higher frequency regime, but they still constitute a relevant approximation of the lattice solution, especially for the lattice-based strain gradient plate solution.

Table 6. Eigenfrequencies Ω of the gradient elasticity and nonlocal plate models compared to the lattice ones—υ = 0.3—case A.

Mode	Eigenmode Numbers and Mode Type			Analytical and Numerical Solutions for Lattice Model, Ω			Local Continuous Plate, Ω
	k_1	k_2	Mode	10 × 10 Cell Lattice	Gradient Elasticity	Nonlocal Elasticity	
1	0	1	shearing	1.851	1.851	1.851	1.859
2	1	0	shearing	1.851	1.851	1.851	1.859
3	1	1	shearing	2.620	2.620	2.620	2.628
4	0	2	shearing	3.656	3.656	3.658	3.717
5	2	0	shearing	3.656	3.656	3.658	3.717
6	1	2	shearing	4.104	4.103	4.105	4.156
7	2	1	shearing	4.104	4.103	4.105	4.156
8	1	1	longitudinal	4.391	4.390	4.391	4.443
9	2	2	shearing	5.188	5.189	5.193	5.257
10	0	3	shearing	5.372	5.366	5.380	5.576

Table 7. Eigenfrequencies Ω of the gradient elasticity and nonlocal plate models compared to the lattice ones—υ = 0.3—case B.

Mode	Eigenmode Numbers and Mode Type			Analytical and Numerical Solutions for Lattice Model, Ω			Local Continuous Plate, Ω
	k_1	k_2	Mode	10 × 10 Cell Lattice	Gradient Elasticity	Nonlocal Elasticity	
1	1	1	shearing	2.620	2.620	2.620	2.628
2	0	1	longitudinal	3.129	3.129	3.129	3.142
3	1	0	longitudinal	3.129	3.129	3.129	3.142
4	1	2	shearing	4.104	4.103	4.105	4.156
5	2	1	shearing	4.104	4.103	4.105	4.156
6	1	1	longitudinal	4.391	4.390	4.391	4.443
7	2	2	shearing	5.188	5.189	5.193	5.257
8	1	3	shearing	5.691	5.683	5.698	5.877
9	3	1	shearing	5.691	5.683	5.698	5.877
10	0	2	longitudinal	6.180	6.179	6.182	6.283

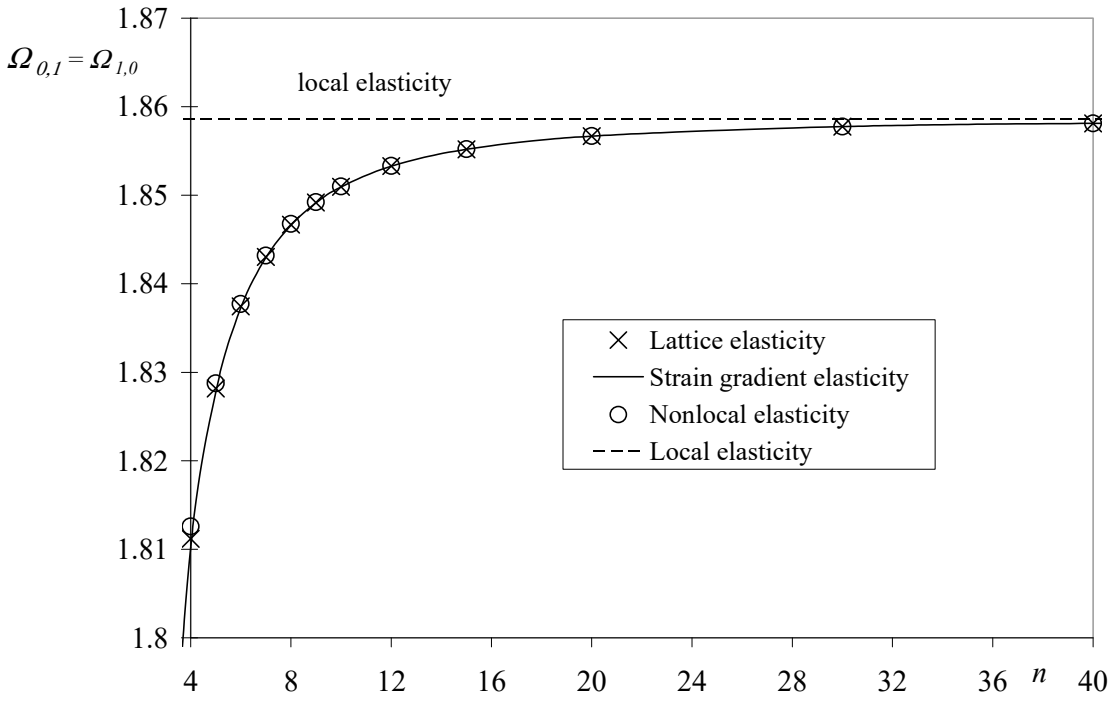

Figure 7. Evolution of the fundamental eigenfrequency $\Omega_{1,0} = \Omega_{0,1}$ of the $n \times n$ cell lattice plate on sliding support—case A (for the in-plane lattice plate problem)—comparison between the exact lattice plate, the strain gradient elastic plate, the nonlocal elastic plate and the continuous local plate models; $\upsilon = 0.3$.

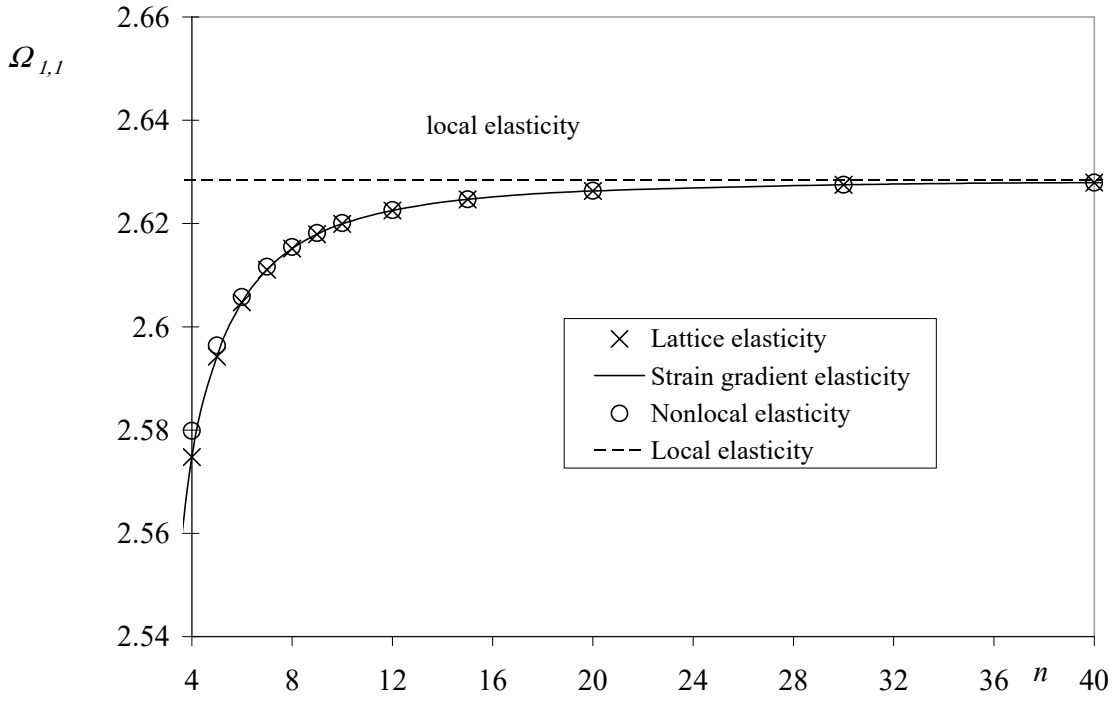

Figure 8. Evolution of the fundamental eigenfrequency $\Omega_{1,1}$ of the $n \times n$ cell lattice plate on sliding support—case B (for the in-plane lattice plate problem)—comparison between the exact lattice plate, the strain gradient elastic plate, the nonlocal elastic plate and the continuous local plate models; $\upsilon = 0.3$.

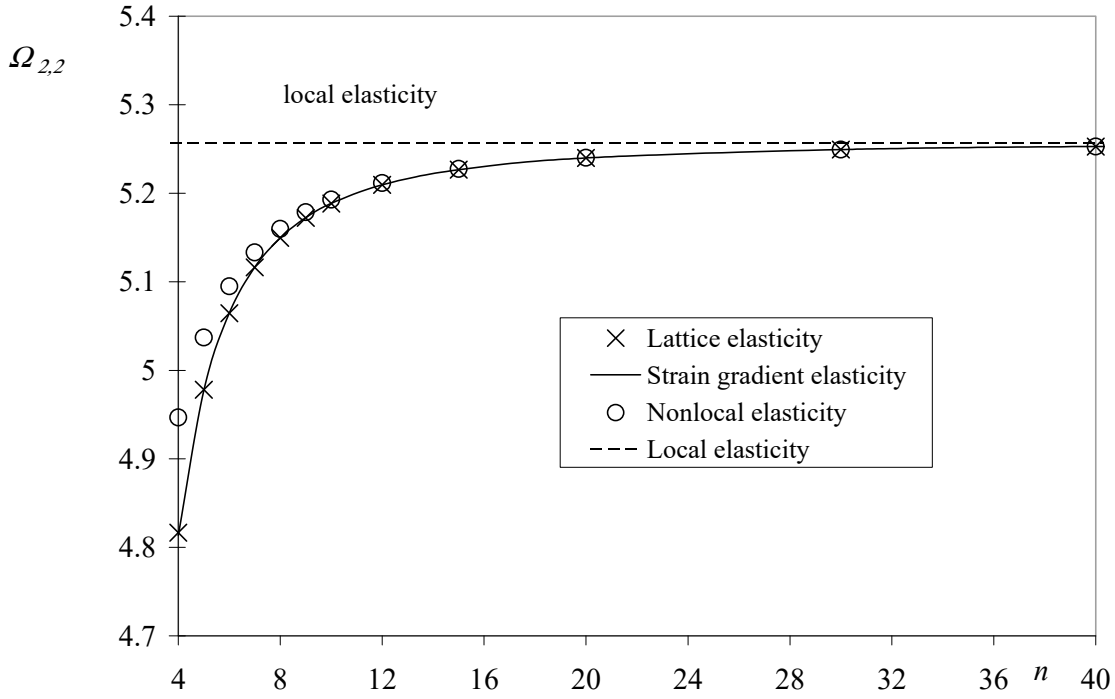

Figure 9. Evolution of the eigenfrequency $\Omega_{2,2}$ of the $n \times n$ cell lattice plate on sliding support—case A (mode 9) or Case B (mode 7) (for the in-plane lattice plate problem)—comparison between the exact lattice plate, the strain gradient elastic plate, the nonlocal elastic plate and the continuous local plate models; $\upsilon = 0.3$.

6. Remarks—Plane Strain

The 2D problem investigated in this paper can be alternatively analysed in plane strain, by comparing the lattice difference equations with those valid for linear elastic isotropy in plane strain:

$$\begin{cases} (\lambda+2\mu)\frac{\partial^2 u}{\partial x^2} + (\lambda+\mu)\frac{\partial^2 v}{\partial x \partial y} + \mu\frac{\partial^2 u}{\partial y^2} + \rho\omega^2 u = 0 \\ (\lambda+2\mu)\frac{\partial^2 v}{\partial y^2} + (\lambda+\mu)\frac{\partial^2 u}{\partial x \partial y} + \mu\frac{\partial^2 v}{\partial x^2} + \rho\omega^2 v = 0 \end{cases} \tag{48}$$

We identify the micro–macro relations for the plane strain analysis:

$$\begin{cases} \alpha = 2\mu h \\ \beta = \lambda h \\ \gamma = \frac{\mu-\lambda}{4} h \end{cases} \tag{49}$$

The eigenfrequencies of the rectangular lattice in plane strain constrained as in cases A and B can be calculated using the same methodology applied in a plane stress framework. For the continuum problem based on Equation (48), the displacement fields in Equation (24) and Equation (25) are assumed for both boundary conditions of cases A and B. Inserting Equation (24) or Equation (25) into Equation (48) gives the eigenfrequency problem for the linear elastic 2D medium in plane strain:

$$\begin{cases} \left[(\lambda+2\mu)\left(\frac{k_1\pi}{L_1}\right)^2 + \mu\left(\frac{k_2\pi}{L_2}\right)^2 - \rho\omega^2\right]U + (\lambda+\mu)\left(\frac{k_1\pi}{L_1}\right)\left(\frac{k_2\pi}{L_2}\right)V = 0 \\ (\lambda+\mu)\left(\frac{k_1\pi}{L_1}\right)\left(\frac{k_2\pi}{L_2}\right)U + \left[(\lambda+2\mu)\left(\frac{k_2\pi}{L_2}\right)^2 + \mu\left(\frac{k_1\pi}{L_1}\right)^2 - \rho\omega^2\right]V = 0 \end{cases} \tag{50}$$

From Equation (50), the eigenfrequencies are solutions of a quartic equation:

$$\left[(\lambda+2\mu)\left(\frac{k_1\pi}{L_1}\right)^2+\mu\left(\frac{k_2\pi}{L_2}\right)^2-\rho\omega^2\right]\left[(\lambda+2\mu)\left(\frac{k_2\pi}{L_2}\right)^2+\mu\left(\frac{k_1\pi}{L_1}\right)^2-\rho\omega^2\right] \\ -(\lambda+\mu)^2\left(\frac{k_1\pi}{L_1}\right)^2\left(\frac{k_2\pi}{L_2}\right)^2=0 \tag{51}$$

which may be presented in the equivalent form:

$$\left(\rho\omega^2\right)^2-(\lambda+3\mu)\left[\left(\frac{k_1\pi}{L_1}\right)^2+\left(\frac{k_2\pi}{L_2}\right)^2\right]\rho\omega^2+\mu(\lambda+2\mu)\left[\left(\frac{k_1\pi}{L_1}\right)^2+\left(\frac{k_2\pi}{L_2}\right)^2\right]^2=0 \tag{52}$$

Equation (52) gives the two families of frequencies in plane strain:

$$\rho\omega^2=\frac{1}{2}[\lambda+3\mu\pm(\lambda+\mu)]\left[\left(\frac{k_1\pi}{L_1}\right)^2+\left(\frac{k_2\pi}{L_2}\right)^2\right] \tag{53}$$

as obtained by Mindlin (2006) [49]. Equation (53) can be also rewritten as:

$$\frac{\omega^2}{c_{shear}^2}=\left[\left(\frac{k_1\pi}{L_1}\right)^2+\left(\frac{k_2\pi}{L_2}\right)^2\right] \text{ or } \frac{\omega^2}{c_{long}^2}=\left[\left(\frac{k_1\pi}{L_1}\right)^2+\left(\frac{k_2\pi}{L_2}\right)^2\right] \tag{54}$$

where we have used the following wave speed valid for the plane strain analysis:

$$c_{shear}=\sqrt{\frac{\mu}{\rho}};\ c_{long}=\sqrt{\frac{\lambda+2\mu}{\rho}} \tag{55}$$

7. Long-Range Interactions

The present analysis, valid for the in-plane vibration of a plane lattice composed of Gazis et al.'s [20] cells, exhibiting central and non-central interactions, can be extended to the vibration of lattices composed of cells exhibiting both short- and long-range interactions, as already investigated by Challamel et al. (2024) [50] for the wave propagation problem in infinite media:

$$\alpha_1\left(u_{i+1,j}-2u_{i,j}+u_{i-1,j}\right)+\alpha_2\left(u_{i+2,j}-2u_{i,j}+u_{i-2,j}\right)+ \\ \frac{\beta_1}{2}\left(u_{i+1,j+1}+u_{i-1,j-1}+u_{i-1,j+1}+u_{i+1,j-1}-4u_{i,j}\right)+\frac{\beta_2}{2}\left(u_{i+2,j+2}+u_{i-2,j-2}+u_{i-2,j+2}+u_{i+2,j-2}-4u_{i,j}\right)+ \\ \left(\frac{\beta_1}{2}+\gamma_1\right)\left(v_{i+1,j+1}-v_{i-1,j+1}-v_{i+1,j-1}+v_{i-1,j-1}\right)+\left(\frac{\beta_2}{2}+\gamma_2\right)\left(v_{i+2,j+2}-v_{i-2,j+2}-v_{i+2,j-2}+v_{i-2,j-2}\right)+ \\ 4\gamma_1\left(u_{i,j+1}-2u_{i,j}+u_{i,j-1}\right)+4\gamma_2\left(u_{i,j+2}-2u_{i,j}+u_{i,j-2}\right)+M\omega^2u_{i,j}=0$$

and

$$\alpha_1\left(v_{i,j+1}-2v_{i,j}+v_{i,j-1}\right)+\alpha_2\left(v_{i,j+2}-2v_{i,j}+v_{i,j-2}\right)+ \\ \frac{\beta_1}{2}\left(v_{i+1,j+1}+v_{i-1,j-1}+v_{i-1,j+1}+v_{i+1,j-1}-4v_{i,j}\right)+\frac{\beta_2}{2}\left(v_{i+2,j+2}+v_{i-2,j-2}+v_{i-2,j+2}+v_{i+2,j-2}-4v_{i,j}\right)+ \\ \left(\frac{\beta_1}{2}+\gamma_1\right)\left(u_{i+1,j+1}-u_{i-1,j+1}-u_{i+1,j-1}+u_{i-1,j-1}\right)+\left(\frac{\beta_2}{2}+\gamma_2\right)\left(u_{i+2,j+2}-u_{i-2,j+2}-u_{i+2,j-2}+u_{i-2,j-2}\right)+ \\ 4\gamma_1\left(v_{i+1,j}-2v_{i,j}+v_{i-1,j}\right)+4\gamma_2\left(v_{i+2,j}-2v_{i,j}+v_{i-2,j}\right)+M\omega^2v_{i,j}=0 \tag{56}$$

where the short-range stiffnesses α_1, β_1, γ_1 are positive to ensure the positive definiteness of the associated short-range energy, and the long-range stiffnesses α_2, β_2, γ_2 are also positive to ensure the positive definiteness of the associated long-range energy. This model can also be understood as a two-cell 2D interaction lattice.

For this generalised lattice problem with two generic interactions in plane stress, we have the possible material calibration:

$$\left\{\begin{array}{l}\alpha_1=\frac{Eh}{1+v}\xi_1\\ \beta_1=\frac{Ehv}{1-v^2}\xi_1\\ \gamma_1=\frac{Eh(1-3v)}{8(1-v^2)}\xi_1\end{array}\right. \text{ and } \left\{\begin{array}{l}\alpha_2=\frac{Eh}{1+v}\frac{\xi_2}{4}\\ \beta_2=\frac{Ehv}{1-v^2}\frac{\xi_2}{4}\\ \gamma_2=\frac{Eh(1-3v)}{8(1-v^2)}\frac{\xi_2}{4}\end{array}\right. \text{ and } \xi_1+\xi_2=1;\ \xi_1\geq 0;\ \xi_2\geq 0 \quad (57)$$

where (ξ_1, ξ_2) are weighting coefficients which control the proportion of short-range to long-range interactions. (ξ_1, ξ_2) = (1, 0) corresponds to a pure short-range interaction problem, as previously studied, whereas (ξ_1, ξ_2) = (0, 1) corresponds to a pure long-range interaction problem.

To investigate its vibration, it is possible for both boundary conditions of cases A and B to assume the modes in Equations (7) and (8), thus leading to the coupled system of linear equations:

$$\left\{\begin{array}{l}\left[\begin{array}{l}4\alpha_1\sin^2\left(\frac{k_1\pi}{2n}\right)+4\alpha_2\sin^2\left(\frac{k_1\pi}{n}\right)+2\beta_1\left[1-\cos\left(\frac{k_1\pi}{n}\right)\cos\left(\frac{k_2\pi}{m}\right)\right]\\ +2\beta_2\left[1-\cos\left(\frac{2k_1\pi}{n}\right)\cos\left(\frac{2k_2\pi}{m}\right)\right]+16\gamma_1\sin^2\left(\frac{k_2\pi}{2m}\right)+16\gamma_2\sin^2\left(\frac{k_2\pi}{m}\right)-M\omega^2\end{array}\right]U\\ +\left[(2\beta_1+4\gamma_1)\sin\left(\frac{k_1\pi}{n}\right)\sin\left(\frac{k_2\pi}{m}\right)+(2\beta_2+4\gamma_2)\sin\left(\frac{2k_1\pi}{n}\right)\sin\left(\frac{2k_2\pi}{m}\right)\right]V=0\\ \left[(2\beta_1+4\gamma_1)\sin\left(\frac{k_1\pi}{n}\right)\sin\left(\frac{k_2\pi}{m}\right)+(2\beta_2+4\gamma_2)\sin\left(\frac{2k_1\pi}{n}\right)\sin\left(\frac{2k_2\pi}{m}\right)\right]U\\ +\left[\begin{array}{l}4\alpha_1\sin^2\left(\frac{k_2\pi}{2m}\right)+4\alpha_2\sin^2\left(\frac{k_2\pi}{m}\right)+2\beta_1\left[1-\cos\left(\frac{k_1\pi}{n}\right)\cos\left(\frac{k_2\pi}{m}\right)\right]\\ 2\beta_2\left[1-\cos\left(\frac{2k_1\pi}{n}\right)\cos\left(\frac{2k_2\pi}{m}\right)\right]+16\gamma_1\sin^2\left(\frac{k_1\pi}{2n}\right)+16\gamma_2\sin^2\left(\frac{k_1\pi}{n}\right)-M\omega^2\end{array}\right]V=0\end{array}\right. \quad (58)$$

The vanishing of the determinant of the system Equation (58) gives the quartic equation for the in-plane eigenfrequencies of rectangular lattices composed of cells with long-range interactions:

$$D_{11}\left(\omega^2\right)D_{22}\left(\omega^2\right)-D_{12}D_{21}=0 \quad (59)$$

with

$$\left\{\begin{array}{l}D_{11}\left(\omega^2\right)=4\alpha_1\sin^2\left(\frac{k_1\pi}{2n}\right)+4\alpha_2\sin^2\left(\frac{k_1\pi}{n}\right)+2\beta_1\left[1-\cos\left(\frac{k_1\pi}{n}\right)\cos\left(\frac{k_2\pi}{m}\right)\right]\\ +2\beta_2\left[1-\cos\left(\frac{2k_1\pi}{n}\right)\cos\left(\frac{2k_2\pi}{m}\right)\right]+16\gamma_1\sin^2\left(\frac{k_2\pi}{2m}\right)+16\gamma_2\sin^2\left(\frac{k_2\pi}{m}\right)-M\omega^2\\ D_{12}=(2\beta_1+4\gamma_1)\sin\left(\frac{k_1\pi}{n}\right)\sin\left(\frac{k_2\pi}{m}\right)+(2\beta_2+4\gamma_2)\sin\left(\frac{2k_1\pi}{n}\right)\sin\left(\frac{2k_2\pi}{m}\right)\\ D_{21}=D_{12}=(2\beta_1+4\gamma_1)\sin\left(\frac{k_1\pi}{n}\right)\sin\left(\frac{k_2\pi}{m}\right)+(2\beta_2+4\gamma_2)\sin\left(\frac{2k_1\pi}{n}\right)\sin\left(\frac{2k_2\pi}{m}\right)\\ D_{22}\left(\omega^2\right)=4\alpha_1\sin^2\left(\frac{k_2\pi}{2m}\right)+4\alpha_2\sin^2\left(\frac{k_2\pi}{m}\right)+2\beta_1\left[1-\cos\left(\frac{k_1\pi}{n}\right)\cos\left(\frac{k_2\pi}{m}\right)\right]\\ 2\beta_2\left[1-\cos\left(\frac{2k_1\pi}{n}\right)\cos\left(\frac{2k_2\pi}{m}\right)\right]+16\gamma_1\sin^2\left(\frac{k_1\pi}{2n}\right)+16\gamma_2\sin^2\left(\frac{k_1\pi}{n}\right)-M\omega^2\end{array}\right. \quad (60)$$

Equation (60) is a quartic equation for long-range, also dubbed as multi-cell, interactions, which generalises the one valid for the in-plane vibration of the rectangular lattices composed of Gazis et al.'s cells [20] exhibiting only short-range, also dubbed as cell-to-cell, interactions.

8. Conclusions

Studied herein is the in-plane vibration problem of rectangular elastic lattice plates. The lattice considered here is a 2D model pioneered by Gazis et al. (1960) [24] and accounts for central and non-central interactions, the latter of the angular type. For sufficiently small spacing, the lattice converges to a linear isotropic elastic continuum, at the asymptotic limit. The rectangular lattice plate is assumed to be constrained by sliding supports along its boundary. The elastic interaction in the vicinity of the boundaries is corrected, as described by Hrennikoff (1941) [41] and McHenry (1943) [40] for central lattices. The exact solutions in terms of eigenfrequencies and eigenmodes are analytically derived for this in-plane discrete plate problem from the resolution of a linear difference eigenvalue problem. We show how

the eigenfrequency spectrum of the rectangular lattice converges to the continuous one (provided by Rayleigh [35]) from below, when the lattice spacing decreases, as usually observed for such spatial finite difference eigenvalue problems. We also developed two lattice-based higher-order continuous plate models to account for the specific scale effects associated with the lattice response. The gradient elasticity model derived herein is built by asymptotic expansion of the lattice difference equations, including central and non-central interactions. The gradient elasticity equations coincide with the ones of Mindlin (1968) [26], even if Mindlin [26] developed the 3D gradient elasticity model from the 3D Gazis et al. lattice model [20], whereas in the present paper we apply the same methodology for the plane stress problem. An exact solution for the eigenfrequencies of the simply supported gradient elasticity plate is also presented, and is shown to accurately fit the lattice response. We also present the exact solutions for a lattice-based nonlocal plate model which avoids the used of higher-order differential operators. The exact eigenfrequency solution for this alternative nonlocal plate model is also derived and compared to the lattice model. Both size-dependent lattice-based plate models accurately capture the scale effects of the in-plane lattice. A possible extension of this work would be to consider more general long-range elastic interactions for the lattice. It would be also interesting to include some additional inner masses (2D or 3D mass-in-mass lattices), as recently studied by Karampour et al. (2024) [51] for simply supported mass-in-mass rectangular lattices.

Author Contributions: Methodology, N.C.; Validation, H.P.N.; Writing—review & editing, C.M.W. and G.R. All authors have read and agreed to the published version of the manuscript.

Funding: This research received no external funding.

Data Availability Statement: Data is contained within the article.

Acknowledgments: Noël Challamel would like to thank Francesco Dell'Isola for stimulating discussions on discrete to continuous modelling in structural mechanics. Giuseppe Ruta acknowledges the financial support of the national grant PRIN PNRR 2022 P2022ATTAR.

Conflicts of Interest: The authors declare no conflict of interest.

References

1. Capecchi, D.; Ruta, G.; Trovalusci, P. From classical to Voigt's molecular models in elasticity. *Arch. Hist. Exact Sci.* **2010**, *64*, 525–559. [CrossRef]
2. Capecchi, D.; Ruta, G.; Trovalusci, P. Voigt and Poincaré's mechanistic-energetic approaches to linear elasticity and suggestions for multiscale modelling. *Arch. Appl. Mech.* **2011**, *81*, 1573–1584. [CrossRef]
3. Challamel, N.; Zhang, Y.P.; Wang, C.M.; Ruta, G.; Dell'Isola, F. Discrete and continuous models of linear elasticity: History and connections. *Contin. Mech. Thermodyn.* **2023**, *35*, 347–391. [CrossRef]
4. Andrianov, I.V.; Awrejcewicz, J.; Danishevskyy, V.V. *Linear and Nonlinear Waves in Microstructured Solids—Homogenization and Asymptotic Approaches*; CRC Press: Boca Raton, FL, USA, 2021.
5. Dell'Isola, F.; Steigmann, D.J. (Eds.) *Discrete and Continuum Models for Complex Metamaterials*; Cambridge University Press: Cambridge, UK, 2020.
6. Wang, C.M.; Zhang, H.; Challamel, N.; Pan, W. *Hencky-Bar-Chain/Net for Structural Analysis*; World Scientific: Singapore, 2020.
7. Lagrange, J.L. Recherches sur la nature et la propagation du son. In *Miscellanea Philosophico-Mathematica Societatis Privatae Taurinensis I*; 2rd Pagination, i-112, 1759 (see also Œuvres, Tome 1, 39-148); Ex Typographia Regia: Turin, Italy, 1759.
8. Lagrange, J.L. *Mécanique Analytique, Paris, 1788*, 3rd ed.; Mallet-Bachelier, Ed.; Imprimeur-Libraire du Bureau des Longitudes, de L'école Polytechnique, de L'école Centrale des Arts et Manufactures: France, Paris, 1853.
9. Rosenau, P. Dynamics of dense lattices. *Phys. Rev. B* **1987**, *36*, 5868–5876. [CrossRef] [PubMed]
10. Andrianov, I.; Awrejcewicz, J. Continuous models for 2D discrete media valid for higher-frequency domain. *Comput. Struct.* **2008**, *86*, 140–144. [CrossRef]
11. Lombardo, M.; Askes, H. Elastic wave dispersion in microstructured membrane. *Proc. R. Soc. Lond. A: Math. Phys. Eng. Sci.* **2010**, *466*, 1789–1807. [CrossRef]
12. Hérisson, B.; Challamel, N.; Picandet, V.; Perrot, A.; Wang, C.M. Static and dynamic behaviors of microstructured membranes within nonlocal mechanics. *J. Eng. Mech.* **2018**, *144*, 04017155. [CrossRef]
13. Chen, F.Y. On modeling and direct solution of certain free vibration systems. *J. Sound Vib.* **1971**, *14*, 57–79. [CrossRef]
14. Tong, P.; Pian, T.H.H.; Bucciarblli, L.L. Mode shapes and frequencies by finite element method using consistent and lumped masses. *Comput. Struct.* **1971**, *1*, 623–638. [CrossRef]

15. Zhang, Z.; Wang, C.M.; Challamel, N. Eringen's length scale coefficient for vibration and buckling of nonlocal rectangular plates with simply supported edges. *J. Eng. Mech.* **2015**, *141*, 04014117. [CrossRef]
16. Challamel, N.; Hache, F.; Elishakoff, I.; Wang, C.M. Buckling and vibration of microstructured rectangular plates considering phenomenological and lattice-based nonlocal continuum models. *Compos. Struct.* **2016**, *149*, 145–156. [CrossRef]
17. Hache, F.; Challamel, N.; Elishakoff, I.; Wang, C.M. Comparison of nonlocal continualization schemes for lattice beams and plates. *Arch. Appl. Mech.* **2017**, *87*, 1105–1138. [CrossRef]
18. Challamel, N.; Wang, C.M.; Zhang, H.; Elishakoff, I. Lattice-based nonlocal elastic structural models. In *Size-Dependent Continuum Mechanics Approaches: Theory & Applications*; Ghavanloo, E., Fazelzadeh, S.A., Marotti de Sciarra, F., Eds.; Springer: Berlin/Heidelberg, Germany, 2021; pp. 1–50.
19. Born, M.; von Kármán, T. On fluctuations in spatial grids. *Phys. Z.* **1912**, *13*, 297–309.
20. Lax, M. E1. The relation between microscopic and macroscopic theories of elasticity. In *Lattice Dynamics*; Wallis, R.F., Ed.; Pergamon Press: New York, NY, USA, 1965; pp. 583–596.
21. Gazis, D.C.; Wallis, R.F. Conditions for rotational invariance of a harmonic lattice. *Phys. Rev.* **1966**, *151*, 578–580, Erratum in *Phys. Rev.* **1967**, *156*, 1038. [CrossRef]
22. Keating, P.N. Effect of invariance requirements on the elastic strain energy of crystals with application to the diamond structure. *Phys. Rev.* **1966**, *145*, 637–645. [CrossRef]
23. Keating, P.N. Relationship between themacroscopic and microscopic theory of crystal elasticity. I. Primitive crystals. *Phys. Rev.* **1966**, *152*, 774–779. [CrossRef]
24. Gazis, D.C.; Herman, R.; Wallis, R.F. Surface elastic waves in cubic crystals. *Phys. Rev.* **1960**, *119*, 533–544. [CrossRef]
25. Challamel, N.; Ruta, G.; Nguyen, H.P.; Wang, C.M.; Zhang, Y.P. On angular and surface interactions in two-dimensional elastic lattices. *Eur. J. Mech. A/Solids* **2024**, *104*, 105176. [CrossRef]
26. Mindlin, R.D. Theories of elastic continua and crystal lattice theories. In *Mechanics of Generalized Continua: Proceedings of the IUTAM-Symposium on the Generalized Cosserat Continuum and the Continuum Theory of dislocations with applications, Freudenstadt and Stuttgart, Germany, 1967*; Kröner, E., Ed.; Springer: Berlin/Heidelberg, Germany, 1968; pp. 312–320.
27. Mindlin, R.D. Lattice theory of shear modes of vibration and torsional equilibrium of simple-cubic crystal plates and bars. *Int. J. Solids Struct.* **1970**, *6*, 725–738. [CrossRef]
28. Fermi, E.; Pasta, P.; Ulam, S.; Tsingou, M. *Studies of the Nonlinear Problems, Technical Report*; Los Alamos National Lab. (LANL): Los Alamos, NM, USA, 1955.
29. Weissert, T.P. *The Genesis of Simulation in Dynamics: Pursuing the Fermi-Pasta-Ulam Problem*; Springer Science & Business Media: Berlin/Heidelberg, Germany, 1997.
30. Dauxois, T.; Peyrard, M.; Ruffo, S. The Fermi–Pasta–Ulam 'numerical experiment': History and pedagogical perspectives. *Eur. J. Phys.* **2005**, *26*, S3. [CrossRef]
31. Dauxois, T.; Peyrard, M. *Physics of Solitons*; Cambridge University Press: Cambridge, UK, 2006.
32. Vainchtein, A. Solitary waves in FPU-type lattices. *Phys. D* **2022**, *434*, 133252. [CrossRef]
33. Potapov, A.I.; Pavlov, I.S.; Gorshkov, K.A.; Maugin, G.A. Nonlinear interaction of solitary waves in a 2D lattice. *Wave Motion* **2002**, *34*, 83–95. [CrossRef]
34. Friesecke, G.; Matthies, K. Geometric solitary waves in a 2D mass-spring lattice. *Discret. Contin. Dyn. Syst.* **2003**, *1*, 105–114. [CrossRef]
35. Strutt, J.W. *The Theory of Sound*; Dover: New York, NY, USA, 1894; Volume I, p. 405.
36. Strutt, J.W. On the free vibration of an infinite plate of homogeneous isotropic elastic matter. *Proc. Lond. Math. Soc.* **1889**, *20*, 225–234.
37. Bardell, N.S.; Langley, R.S.; Dunsdon, J.M. On the free in-plane vibration of isotropic rectangular plates. *J. Sound Vib.* **1996**, *191*, 459–467. [CrossRef]
38. Gorman, D.J. Exact solutions for the free in-plane vibration of rectangular plates with two opposite edges simply supported. *J. Sound Vib.* **2006**, *294*, 131–161. [CrossRef]
39. Challamel, N.; Atanackovic, T.; Zhang, Y.P.; Wang, C.M. A fractional nonlocal elastic model for lattice wave analysis. *Mech. Res. Comm.* **2022**, *126*, 103999. [CrossRef]
40. McHenry, D. A lattice analogy for the solution of stress problems. *J. Inst. Civ. Eng.* **1943**, *2*, 59–82. [CrossRef]
41. Hrennikoff, A. Solutions of problems of elasticity by the framework method. *J. Appl. Mech.* **1941**, *8*, A169–A175. [CrossRef]
42. Cauchy, A. Sur les différences finies et les intégrales aux différences des fonctions entières d'une on de plusieurs variables. *Exerc. De Mathématiques* **1828**, 155–159.
43. Collatz, L. *The Numerical Treatment of Differential Equations*; Springer: Berlin/Heidelberg, Germany, 1960.
44. Challamel, N.; Picandet, V.; Collet, B.; Michelitsch, T.; Elishakoff, I.; Wang, C.M. Revisiting finite difference and finite element methods applied to structural mechanics within enriched continua. *Eur. J. Mech. A/Solids* **2015**, *53*, 107–120. [CrossRef]
45. Polya, G. Sur une interprétation de la méthode des différences finies qui peut fournir des bornes supérieures ou inférieures. *C.R. Acad. Sci.* **1952**, *235*, 995–997.
46. Challamel, N.; Wang, C.M.; Elishakoff, I. Nonlocal or gradient elasticity macroscopic models: A question of concentrated or distributed microstructure. *Mech. Res. Commun.* **2016**, *71*, 25–31. [CrossRef]

47. Zhang, Y.P.; Challamel, N.; Wang, C.M. Modelling nano-plane structures with body force using Hencky bar-grid model, continualised nonlocal model and Eringen nonlocal model. *Contin. Mech. Thermodyn.* **2021**, *33*, 2453–2480. [CrossRef]
48. Eringen, A.C. On differential equations of nonlocal elasticity and solutions of screw dislocation and surface waves. *J. Appl. Phys.* **1983**, *54*, 4703–4710. [CrossRef]
49. Mindlin, R.D. *An Introduction to the Mathematical Theory of Vibrations of Elastic Plates*; Yang, J., Ed.; World Scientific: Singapore, 2006.
50. Challamel, N.; Nguyen, H.P.; Ruta, G.; Wang, C.M.; Zhang, Y.P. Meta-truss and generalized elastic lattices with long-range interactions. In *Dynamics of Discrete and Continuum Structures and Media*; Altenbach, H., Eremeyev, V., Eds.; Springer: Berlin/Heidelberg, Germany, 2024; in Press.
51. Karampour, S.; Ghavanloo, E.; Fazelzadeh, S.A. In-plane vibration characteristics of metamaterial plates with locally resonant microstructures. *Acta Mech.* **2024**, *235*, 819–831. [CrossRef]

Disclaimer/Publisher's Note: The statements, opinions and data contained in all publications are solely those of the individual author(s) and contributor(s) and not of MDPI and/or the editor(s). MDPI and/or the editor(s) disclaim responsibility for any injury to people or property resulting from any ideas, methods, instructions or products referred to in the content.